Dynamics of the vitreous humour induced by eye rotations: implications for retinal detachment and intra-vitreal drug delivery

Rodolfo Repetto

Department of Civil, Architectural and Environmental Engineering
University of Genoa, Italy
rodolfo.repetto@unige.it
http://dicat.unige.it/rrepetto/

January 23, 2012

Main collaborators

- **Jennifer Siggers** Imperial College London;
- **Alessandro Stocchino** DICAT, Univeristy of Genoa;
- **Julia Meskauskas** DISAT, University of L'Aquila;
- **Andrea Bonfiglio** DICAT, Univeristy of Genoa.

Anatomy of the eye

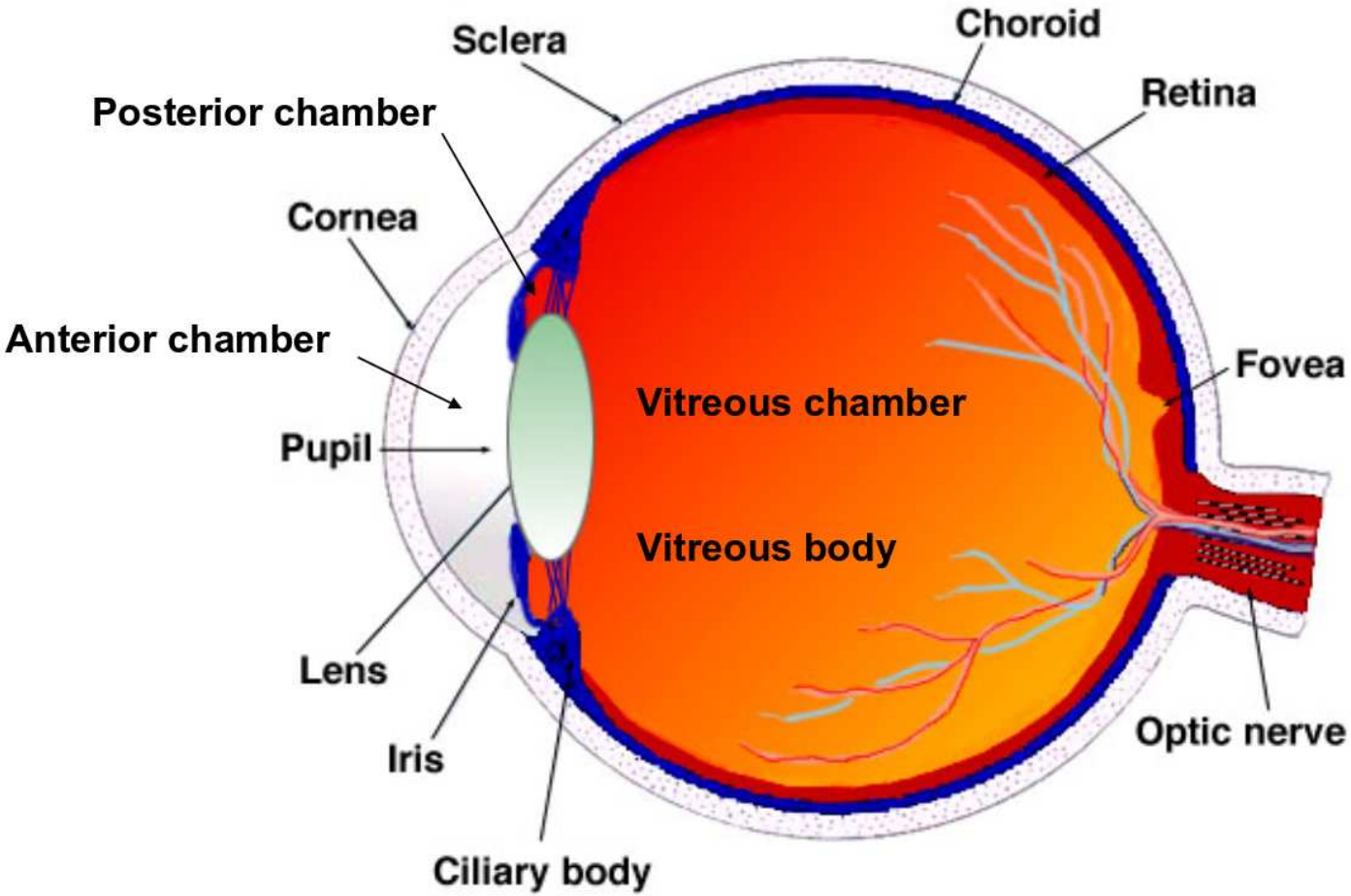

Vitreous characteristics and functions

Vitreous composition

The main constituents are

- Water (99%);
- hyaluronic acid (HA);
- collagen fibrils.

Its structure consists of long, thick, non-branching collagen fibrils suspended in hyaluronic acid.

Normal vitreous characteristics

- The healthy vitreous in youth is a gel-like material with **visco-elastic mechanical properties**, which have been measured by several authors (Lee et al., 1992; Nickerson et al., 2008; Swindle et al., 2008).
- In the outermost part of the vitreous, named **vitreous cortex**, the concentration of collagen fibrils and HA is higher.
- The vitreous cortex is in contact with the **Internal Limiting Membrane (ILM)** of the retina.

Physiological roles of the vitreous

- **Support function for the retina** and filling-up function for the vitreous body cavity;
- **diffusion barrier** between the anterior and posterior segment of the eye;
- establishment of an **unhindered path of light.**

Vitreous ageing

With advancing age the vitreous typically undergoes significant changes in structure.

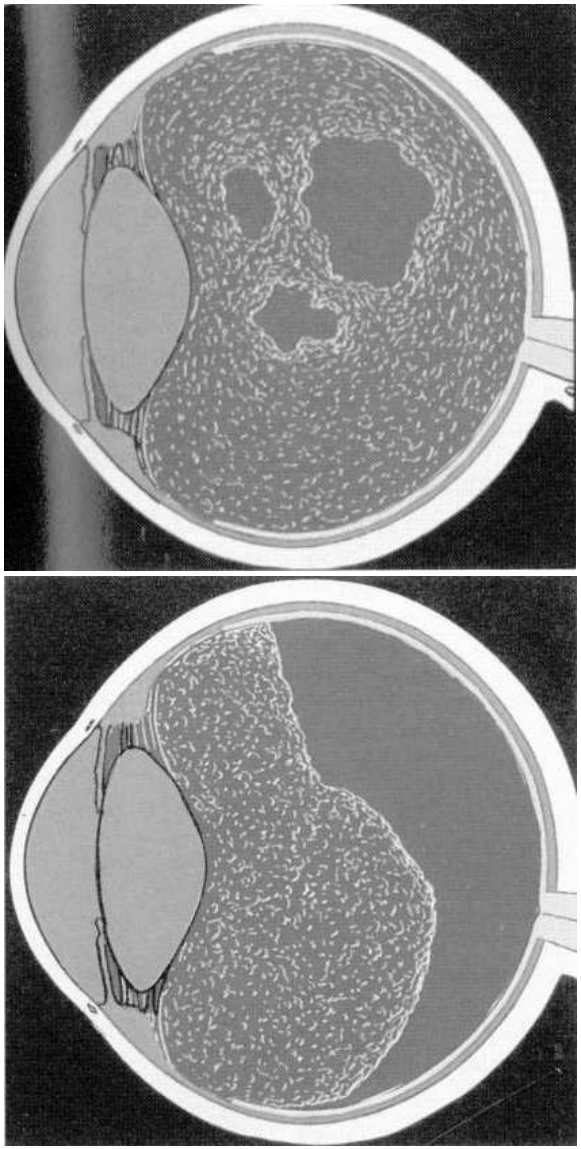

- Disintegration of the gel structure which leads to **vitreous liquefaction (synchisys)**. This leads to an approximately linear increase in the volume of liquid vitreous with time. Liquefaction can be as much extended as to interest the whole vitreous chamber.
- Shrinking of the vitreous gel **(syneresis)** leading to the detachment of the gel vitreous from the retina in certain regions of the vitreous chamber. This process typically occurs in the posterior segment of the eye and is called **posterior vitreous detachment (PVD)**. It is a pathophysiologic condition of the vitreous.

Vitreous replacement

After surgery **(vitrectomy)** the vitreous may be completely replaced with tamponade fluids:

- silicon oils water;
- aqueous humour;
- perfluoropropane gas;
- ...

Partial vitreous liquefaction

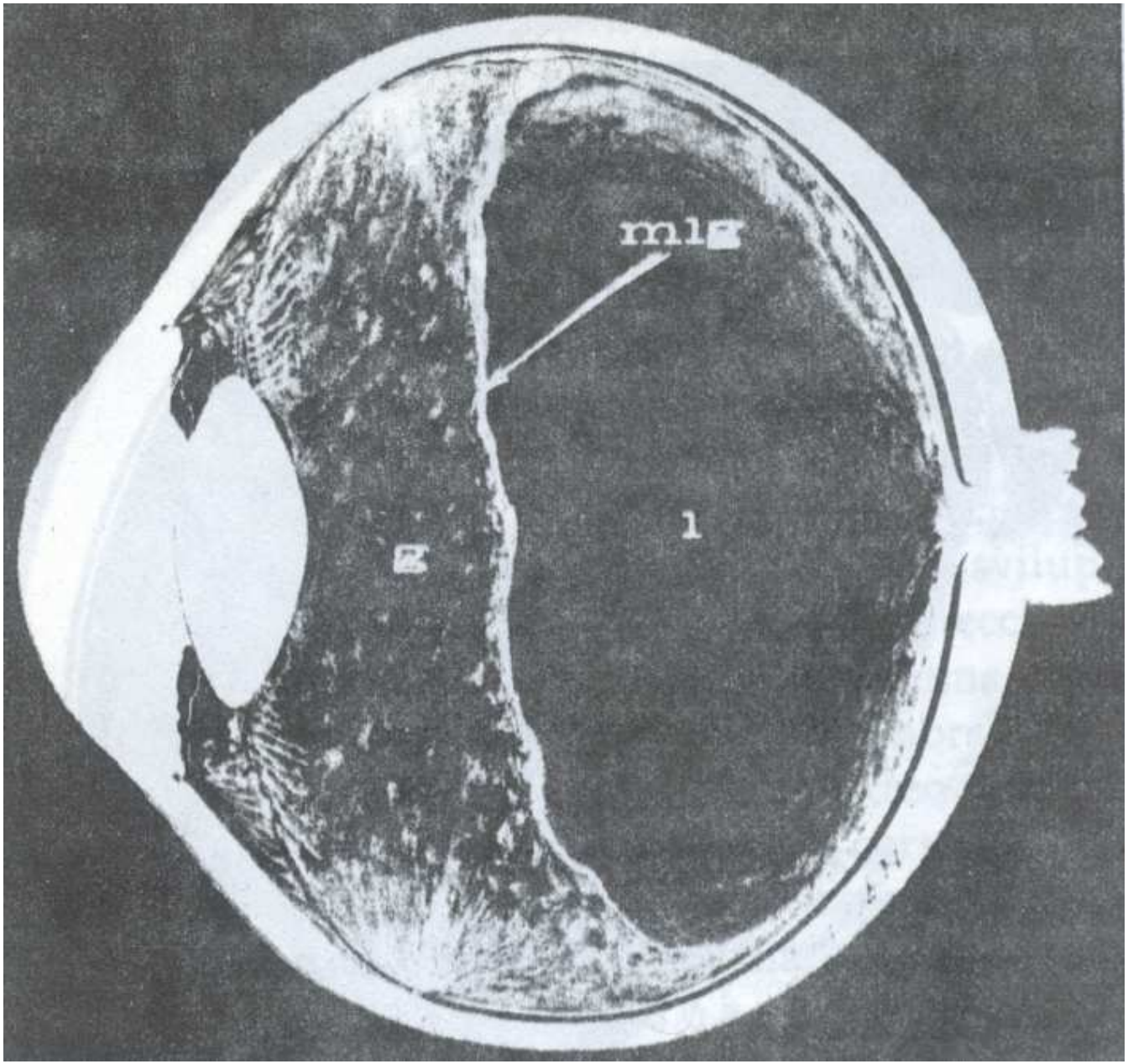

Motivations of the work

Why research on vitreous motion?

- Possible connections between the mechanism of **retinal detachment** and
  - the shear stress on the retina;
  - flow characteristics.
- Especially in the case of liquefied vitreous eye rotations may produce effective **fluid mixing**. In this case **advection may be more important that diffusion** for mass transport within the vitreous chamber.
  Understanding diffusion/dispersion processes in the vitreous chamber is important to predict the behaviour of drugs directly injected into the vitreous.

Retinal detachment

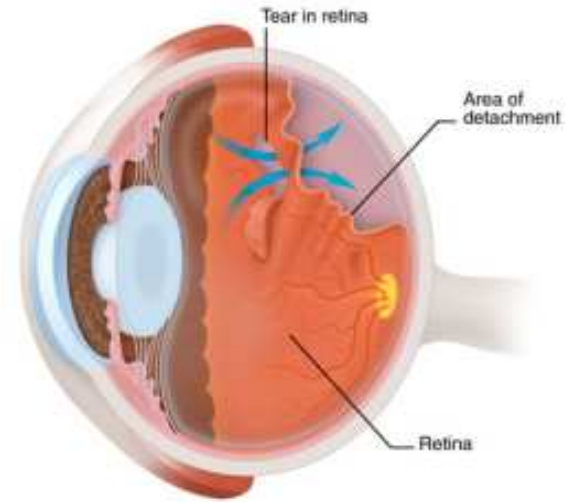

Posterior vitreous detachment and vitreous degeneration:

- more common in myopic eyes;
- preceded by changes in vitreous macromolecular structure and in vitreoretinal interface $\rightarrow$ possibly mechanical reasons.

- If the retina detaches from the underlying layers $\rightarrow$ loss of vision;
- Rhegmatogeneous retinal detachment: fluid enters through a retinal break into the subretinal space and peels off the retina.
- **Risk factors:**
  - **myopia;**
  - posterior vitreous detachment (PVD);
  - lattice degeneration;
  - ...

Scleral buckling

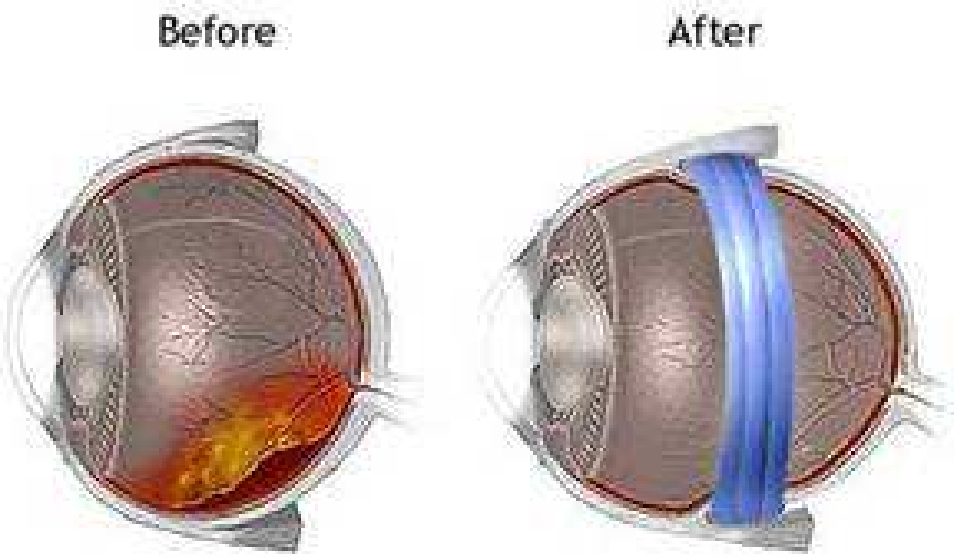

Scleral buckling is the application of a rubber band around the eyeball at the site of a retinal tear in order to promote reachtachment of the retina.

Intravitreal drug delivery

It is difficult to transport drugs to the retina from 'the outside' due to the tight blood-retinal barrier $\rightarrow$ use of **intravitreal drug injections.**

Saccadic eye rotations

Saccades are eye movements that rapidly redirect the eyes from one target to another
The main characteristics of a saccadic eye movement are (Becker, 1989):

- an **extremely intense angular acceleration** (up to 30000 deg/s2);
- a comparatively less intense deceleration which is nevertheless able to induce a very fast arrest of the rotation
- an **angular peak velocity** increasing with the saccade amplitude up to a saturation value **ranging between 400 - 600 deg/s**.

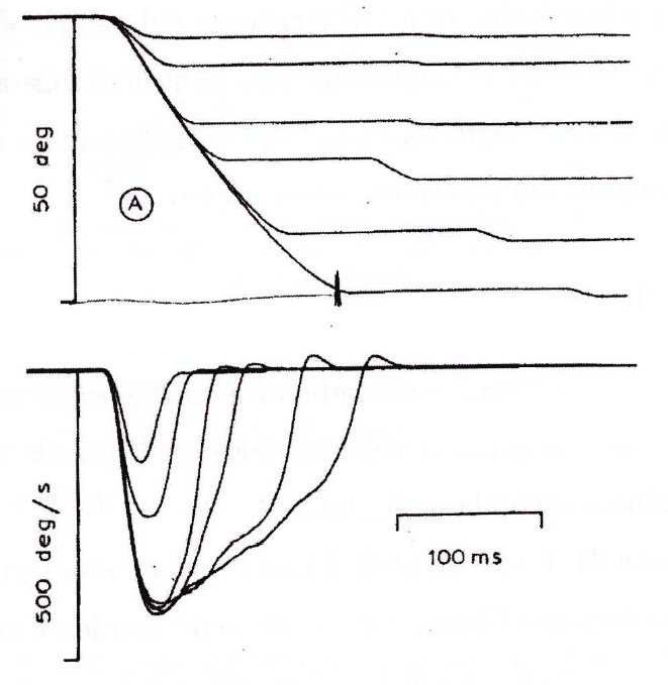

The maximum amplitude of a saccade is about 50° though most eye rotations have amplitudes smaller than 20°. Saccade duration and amplitude are related and the duration is at most of the order of a tenth of a second.

A simple irrotational model

Non-sphericity of the domain

- The antero-posterior axis is shorted than the others;
- the lens produces an anterior indentation.

This effect may have important fluid dynamics consequences.

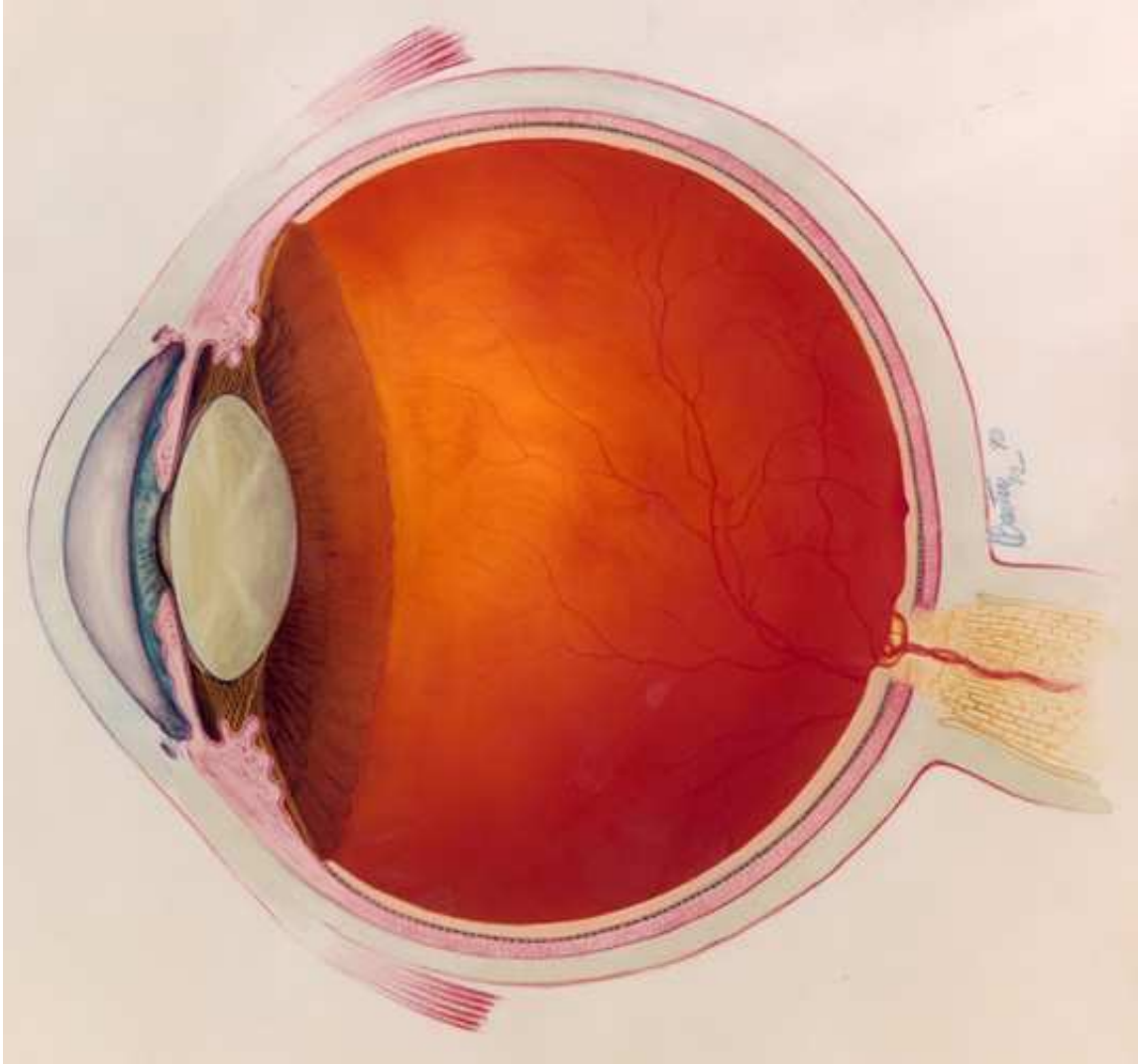

Formulation of the problem I

Repetto et al. (2005), Meccanica.

Assumptions

- We consider a **Newtonian fluid of small viscosity**. This applies to the case of **liquefied vitreous**.
- We assume the vitreous is not moving at the initial time.
- **Fast short-duration eye rotations.**
  In this case the thickness Δ of the boundary layer generated at the wall is of order

$$\Delta \approx \sqrt{\nu t},$$

  where ν is the kinematic viscosity and t is time.

  If for the considered duration of the eye movement we have

$$\Delta \ll R_0,$$

  with R_0 characteristic size of the domain, then **the motion in the core can be considered irrotational**

Formulation of the problem II

The **velocity potential** Φ^* is defined as

$$\mathbf{u}^* = \nabla \Phi^*,$$

where $\mathbf{u}^*$ denotes velocity. **Fluid incompressibility** implies that the velocity potential must be a harmonic function, i.e.

$$\nabla^2 \Phi^* = 0.$$

Considered geometry

Equation of the boundary of the domain

$$r^* = R^*(\vartheta, \phi, t^*)$$

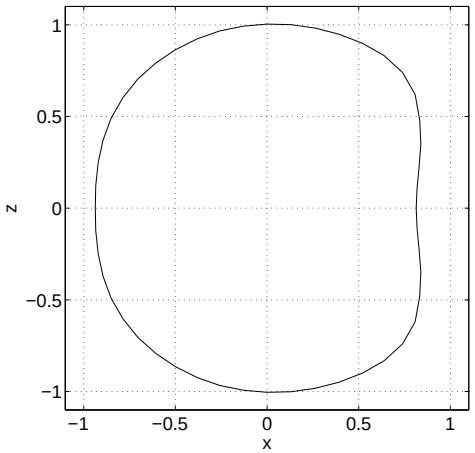

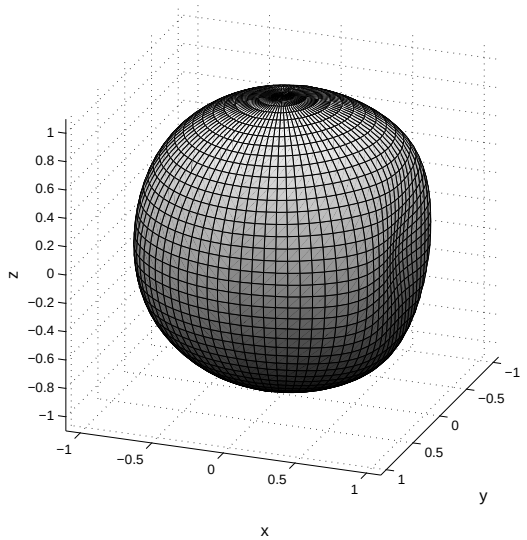

Formulation of the problem III

The mathematical problem is formulated referring to a **fixed frame** and employing a **system of polar spherical coordinates** (r^*, ϑ, ϕ).

Boundary conditions impose **vanishing flux through the eye wall.**

Governing equations

$$\frac{\partial}{\partial r^*}\left(r^{*2}\frac{\partial \Phi}{\partial r^*}\right) + \frac{1}{\sin\vartheta}\frac{\partial}{\partial \vartheta}\left(\sin\vartheta\frac{\partial \Phi^*}{\partial \vartheta}\right) + \frac{1}{\sin^2\vartheta}\frac{\partial^2 \Phi^*}{\partial \phi^2} = 0, \tag{1a}$$

$$-\frac{\partial R^*}{\partial t^*} + \frac{\partial \Phi^*}{\partial r^*} - \frac{1}{r^{*2}}\frac{\partial \Phi^*}{\partial \vartheta}\frac{\partial R^*}{\partial \vartheta} - \frac{1}{r^{*2}\sin^2\vartheta}\frac{\partial \Phi^*}{\partial \phi}\frac{\partial R^*}{\partial \phi} = 0 \qquad [r^* = R^*(\vartheta, \phi - \alpha(t^*))] \tag{1b}$$

$$p^* = -\rho\frac{\partial \Phi^*}{\partial t^*} - \frac{1}{2}\rho\left[\left(\frac{\partial \Phi^*}{\partial r^*}\right)^2 + \left(\frac{1}{r^*}\frac{\partial \Phi^*}{\partial \vartheta}\right)^2 + \left(\frac{1}{r^*\sin\vartheta}\frac{\partial \Phi^*}{\partial \phi}\right)^2\right], \tag{1c}$$

where $\alpha(t^*)$ denotes the **angle of rotation of the globe** with respect to a reference position.

Formulation of the problem IV

Scaling

$$(r, R) = \frac{(r^*, R^*)}{\mathcal{R}}, \quad \Phi = \frac{\Phi^*}{\Omega_p \mathcal{R}^2}, \quad p = \frac{p^*}{\rho \Omega_p^2 \mathcal{R}^2}, \quad t = \Omega_p t^*, \tag{2}$$

where

- $\mathcal{R}$: radius of the sphere with the same volume as the actual domain;
- Ω_p: peak angular velocity of the saccadic movement.

Change of coordinates

We introduce the coordinate

$$\varphi = \phi - \alpha(t), \tag{3}$$

so that the position of the eye wall is no longer time-dependent.
Using the above scalings and (3) equations (1a), (1b) and (1c) can be written as

$$\frac{\partial}{\partial r}\left(r^2 \frac{\partial \Phi}{\partial r}\right) + \frac{1}{\sin\vartheta}\frac{\partial}{\partial \vartheta}\left(\sin\vartheta \frac{\partial \Phi}{\partial \vartheta}\right) + \frac{1}{\sin^2\vartheta}\frac{\partial^2 \Phi}{\partial \varphi^2} = 0, \tag{4a}$$

$$\dot{\alpha}\frac{\partial R}{\partial \varphi} + \frac{\partial \Phi}{\partial r} - \frac{1}{r^2}\frac{\partial \Phi}{\partial \vartheta}\frac{\partial R}{\partial \vartheta} - \frac{1}{r^2 \sin^2\vartheta}\frac{\partial \Phi}{\partial \varphi}\frac{\partial R}{\partial \varphi} = 0 \qquad [r = R(\vartheta, \varphi)], \tag{4b}$$

$$\frac{\partial \Phi}{\partial t} - \dot{\alpha}\frac{\partial \Phi}{\partial \varphi} + p + \frac{1}{2}\left[\left(\frac{\partial \Phi}{\partial r}\right)^2 + \left(\frac{1}{r}\frac{\partial \Phi}{\partial \vartheta}\right)^2 + \left(\frac{1}{r\sin\vartheta}\frac{\partial \Phi}{\partial \varphi}\right)^2\right] = 0, \tag{4c}$$

where the superscript dot denotes derivatives with respect to the dimensionless time.

Formulation of the problem V

Shape of the domain

We describe the eye globe of as a **slightly deformed sphere** writing

$$R(\vartheta, \varphi) = 1 + \delta R_1(\vartheta, \varphi),$$

where $\delta \ll 1$ represents the maximum departure of the domain from the unit sphere.

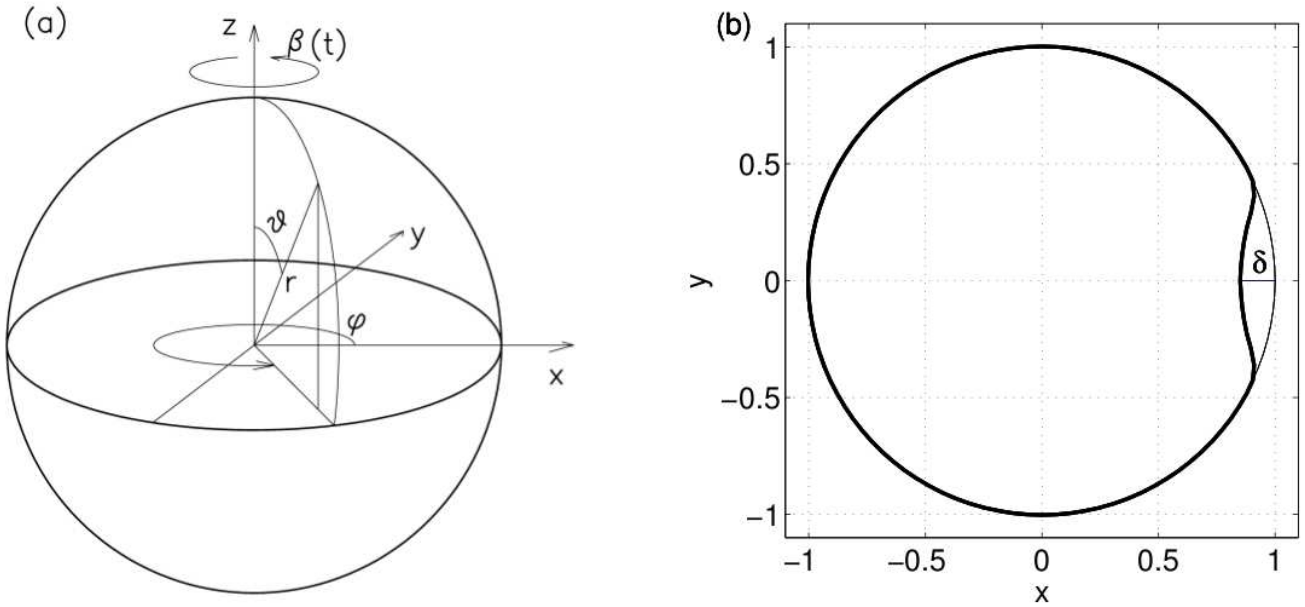

Formulation of the problem VI

Expansion

The function $R_1(\vartheta, \varphi)$ can be expanded in terms of **spherical harmonics**

$$R_1 = \sum_{m=0}^{\infty} \sum_{n=m}^{\infty} a_{mn} \cos(m\varphi) P_n^m(\cos\vartheta), \tag{5}$$

where P_n^m are the **associated Legendre functions**, defined in terms of the **Legendre polynomials** P_n as follows

$$P_n^m(x) = (1 - x^2)^{m/2} \frac{d^m}{dx^m} P_n(x).$$

Note: as the domain is symmetrical with respect to the plane $y = 0$, only the symmetrical Fourier modes $(\cos m\varphi)$ have been included in the expansion (5).

Taking advantage of the **orthogonality properties of the associated Legendre functions**, the coefficients a_{mn} appearing in (5) can be computed as

$$a_{mn} = \frac{k_m (2n+1)(n-m)!}{4\pi(n+m)!} \int_0^{2\pi} \int_0^{\pi} R_1(\vartheta, \varphi) \cos(m\varphi) P_n^m(\cos\vartheta) \sin\vartheta \; d\vartheta \; d\varphi,$$

$$k_0 = 1, \qquad k_m = 2 \quad (m > 0).$$

Solution I

Expansion in terms of δ

In physiological conditions $0.15 \lessapprox \delta \lessapprox 0.2$. This suggests to expand Φ and p in powers of δ

$$\Phi = \Phi_0 + \delta\Phi_1 + \mathcal{O}(\delta^2), \tag{6a}$$

$$p = p_0 + \delta p_1 + \mathcal{O}(\delta^2). \tag{6b}$$

Leading order problem $\mathcal{O}(\delta^0)$

At leading order we find the trivial solution

$$\Phi_0 = 0, \qquad p_0 = \text{const.}$$

No motion is generated in a fluid filling a rotating sphere if the no slip condition at the wall is not imposed.

Solution II

Order δ problem

At order δ the governing equations (4a), (4b) and (4c) reduce to

$$\nabla^2 \Phi_1 = 0, \tag{7a}$$

$$\frac{\partial \Phi_1}{\partial r} = -\dot{\alpha} \frac{\partial R_1}{\partial \varphi} \qquad (r = 1), \tag{7b}$$

$$p_1 = -\frac{\partial \Phi_1}{\partial t} + \dot{\alpha} \frac{\partial \Phi_1}{\partial \varphi}. \tag{7c}$$

Equation (5) and the boundary condition (7b) suggest to expand the function Φ_1 as follows

$$\Phi_1 = \sum_{m=0}^{\infty} \sum_{n=m}^{\infty} \Phi_{mn}(r) \sin(m\varphi) P_n^m(\cos\vartheta).$$

Substituting into the equations (7a) and (7b), we obtain the following ODE

$$\frac{d}{dr}\left(r^2 \frac{d\Phi_{mn}}{dr}\right) - n(n+1)\Phi_{mn} = 0,$$

$$\frac{d\Phi_{mn}}{dr} = a_{mn}\dot{\alpha} m, \qquad (r = 1),$$

with regularity conditions at the origin.

Solution III

Order δ solution

$$\Phi_{mn} = a_{mn}\dot{\alpha}\frac{m}{n}r^n.$$

Hence, the order δ **velocity components** read

$$u_{r1} = \sum_{m=0}^{\infty}\sum_{n=m}^{\infty} a_{mn}\dot{\alpha}mr^{n-1}\sin(m\varphi)P_n^m(\cos\vartheta),$$

$$u_{\vartheta 1} = \sum_{m=0}^{\infty}\sum_{n=m}^{\infty} a_{mn}\dot{\alpha}\frac{m}{n}r^{n-1}\sin(m\varphi)\frac{d}{d\vartheta}P_n^m(\cos\vartheta),$$

$$u_{\varphi 1} = \sum_{m=0}^{\infty}\sum_{n=m}^{\infty} \frac{a_{mn}\dot{\alpha}\frac{m^2}{n}r^{n-1}\cos(m\varphi)P_n^m(\cos\vartheta)}{\sin\vartheta}.$$

From the linearised Bernoulli equation (7c) we find the pressure as

$$p_1 = \sum_{m=0}^{\infty}\sum_{n=m}^{\infty} -a_{mn}\ddot{\alpha}\frac{m}{n}r^n\sin(m\varphi)P_n^m(\cos\vartheta) + a_{mn}\dot{\alpha}^2\frac{m^2}{n}r^n\cos(m\varphi)P_n^m(\cos\vartheta).$$

Results I

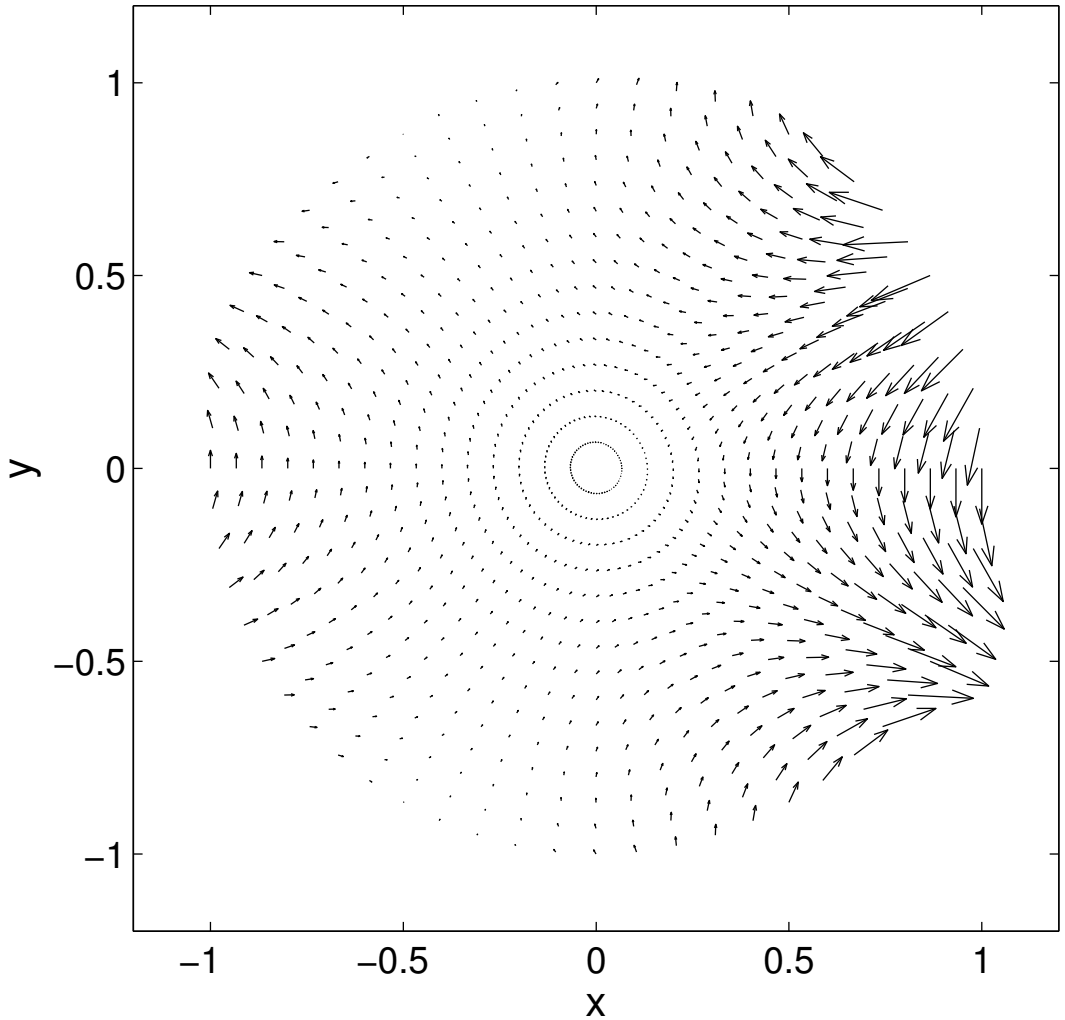

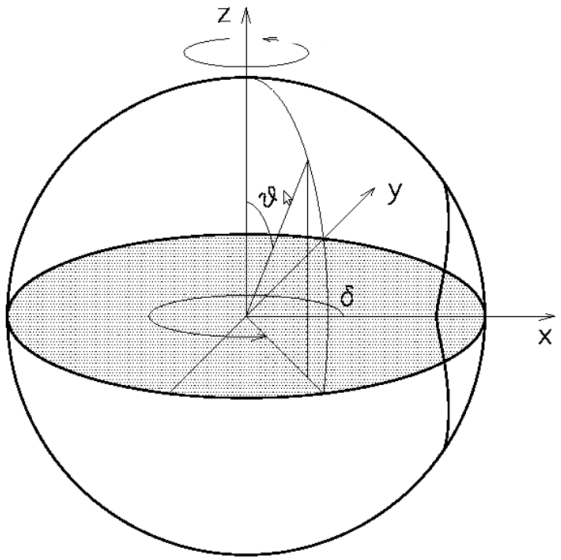

Velocity field on the equatorial plane induced by a counterclockwise rotation.

Results II

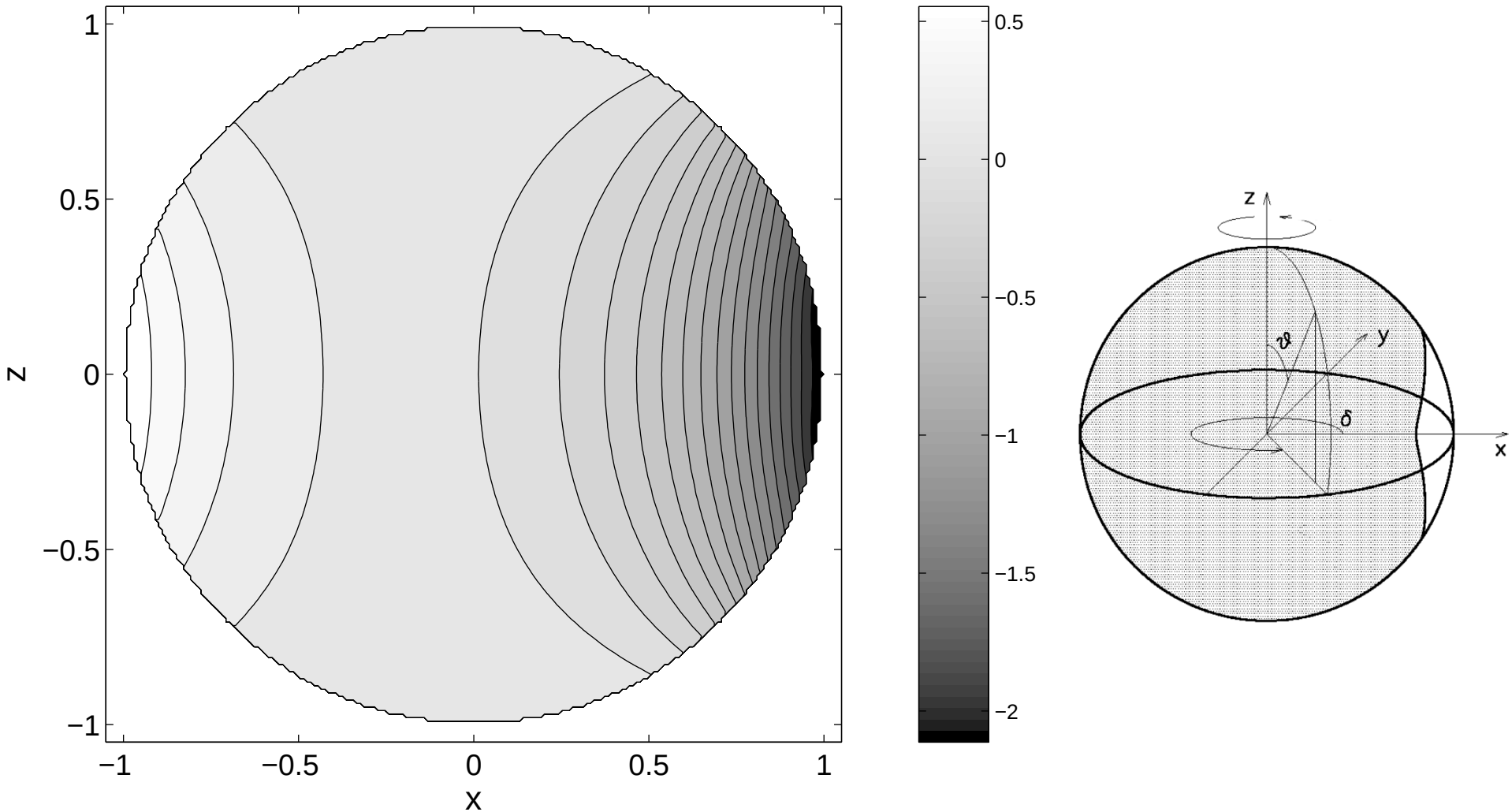

Contours of the out-of-plane velocity magnitude on the vertical plane of symmetry.

Results III

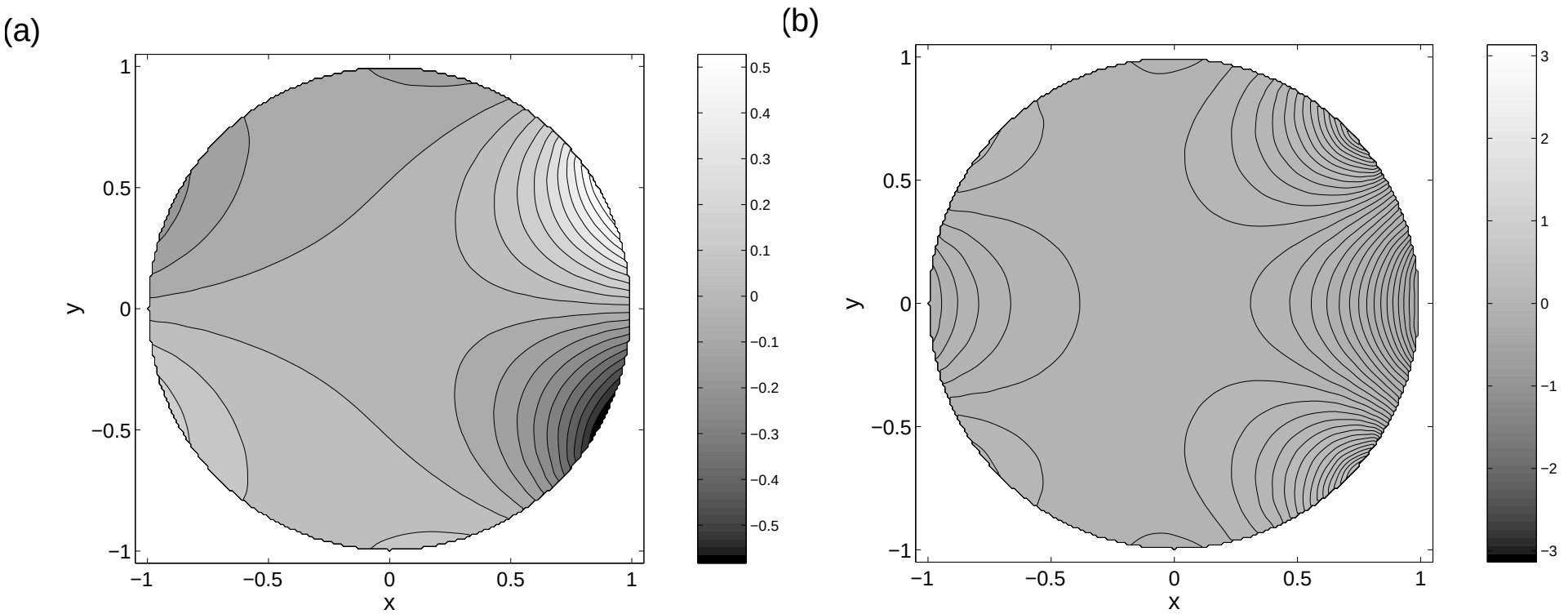

Pressure field on the equatorial plane.

- (a) time of maximum angular acceleration.
- (b) time of maximum angular velocity.

Some preliminary conclusions

- This simple model suggests that, especially in the case of low viscosity fluids, **the shape of the vitreous chamber plays a significant role in vitreous motion.**
- The flow field is complex and significantly three-dimensional.
- A circulation is likely to form in the anterior part on the vitreous chamber, close to the lens.

The effect of viscosity

Main working assumptions

- **Newtonian fluid**
  The assumption of purely viscous fluid applies to the cases of
  - vitreous liquefaction;
  - substitution of the vitreous with viscous tamponade fluids .
- **Sinusoidal eye rotations**
  Using dimensional analysis it can be shown that the problem is governed by the following two dimensionless parameters

$$\alpha = \sqrt{\frac{R_0^2 \omega_0}{\nu}}$$ **Womersley number**,

ε **Amplitude of oscillations**.

- **Spherical domain**

Theoretical model I

David et al. (1998)

Scalings

$$\mathbf{u} = \frac{\mathbf{u}^*}{\omega_0 R_0}, \quad t = t^* \omega_0, \quad r = \frac{r^*}{R_0}, \quad p = \frac{p^*}{\mu \omega_0},$$

where ω_0 denotes the angular frequency of the domain oscillations, R_0 the sphere radius and μ the dynamic viscosity of the fluid.

Dimensionless equations

$$\alpha^2 \frac{\partial}{\partial t}\mathbf{u} + \alpha^2 \mathbf{u} \cdot \boldsymbol{\nabla}\mathbf{u} + \boldsymbol{\nabla} p - \nabla^2 \mathbf{u} = 0, \qquad \boldsymbol{\nabla} \cdot \mathbf{u} = 0, \tag{8}$$

$$u = v = 0, \quad w = \varepsilon \sin\vartheta \sin t \qquad (r = 1), \tag{9}$$

where ε is the amplitude of oscillations. **We assume $\varepsilon \ll 1$.**

Asymptotic expansion

$$\mathbf{u} = \varepsilon \mathbf{u}_1 + \varepsilon^2 \mathbf{u}_2 + \mathcal{O}(\varepsilon^3), \quad p = \varepsilon p_1 + \varepsilon^2 p_2 + \mathcal{O}(\varepsilon^3).$$

Since the equations and boundary conditions for u_1, v_1 and p_1 are homogeneous the solution is $p_1 = u_1 = v_1 = 0$.

Theoretical model II

The **leading order azimuthal component of the velocity** w_1 satisfies the equation

$$\frac{\partial w_1}{\partial t} = \frac{1}{\alpha^2}\left[\frac{1}{r^2}\frac{\partial}{\partial r}\left(r^2\frac{\partial w_1}{\partial r}\right) + \frac{1}{r^2\sin\vartheta}\frac{\partial}{\partial\vartheta}\left(\sin\vartheta\frac{\partial w_1}{\partial\vartheta}\right) - \frac{w_1}{r^2\sin^2\vartheta}\right],$$

$$w_1 = \sin\vartheta\sin t \qquad (r=1).$$

Separate variable solution

$$w_1 = g_1(r)e^{it}\sin\vartheta + c.c.$$

Ordinary differential equation

$$r^2 g_1'' + 2rg_1' - \left(2 + ir^2\alpha^2\right) g_1 = 0.$$

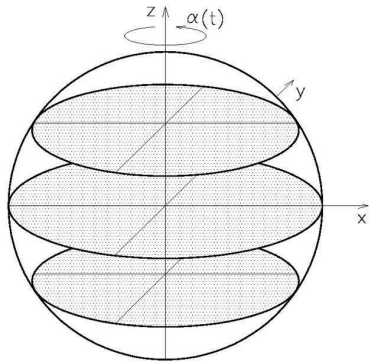

Solution

$$w_1 = g_1(r)e^{it}\sin\vartheta + c.c., \quad g_1(r) = -\frac{i}{2r^2}\left(\frac{\sin kr - kr\cos kr}{\sin k - k\cos k}\right), \quad k = e^{-i\pi/4}\alpha.$$

where $c.c.$ denotes the complex conjugate.

Theoretical model III

Velocity profiles on the plane orthogonal to the axis of rotation at different times.

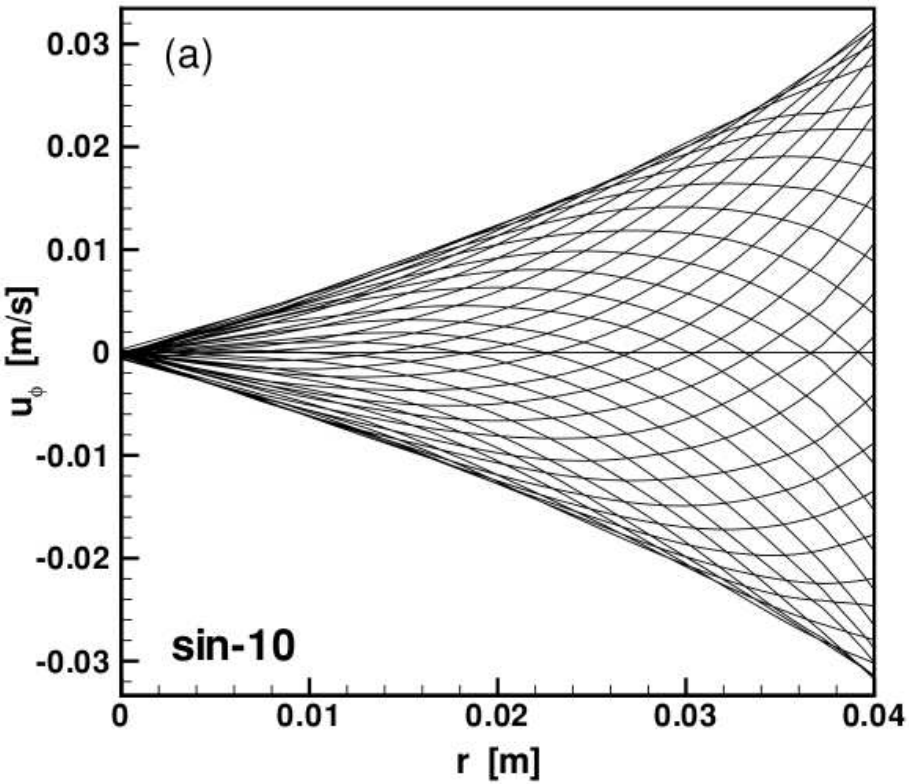

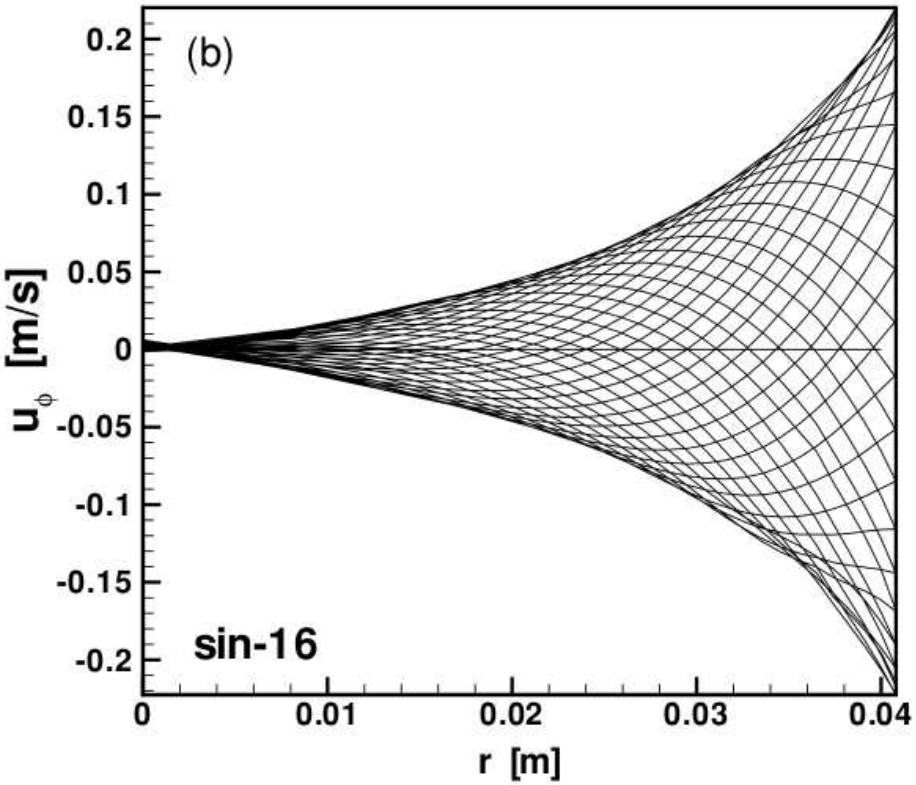

- Limit of small α: **rigid body rotation;**
- Limit of large α: formation of an **oscillatory boundary layer at the wall.**

Experimental apparatus I

Repetto et al. (2005), Phys. Med. Biol.
The experimental apparatus is located at the University of Genoa.

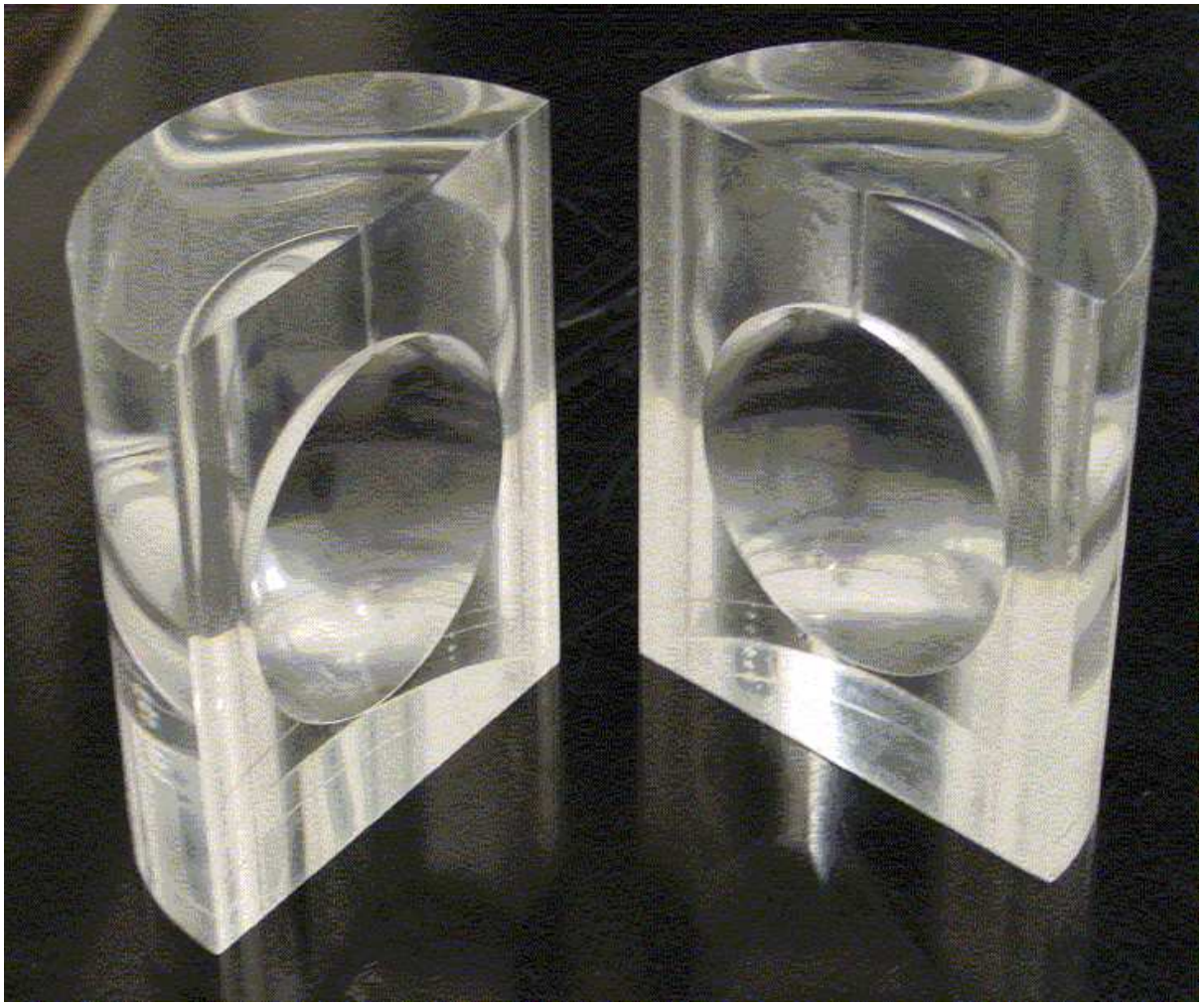

- Perspex cylindrical container.
- Spherical cavity with radius $R_0 = 40$ mm.
- Glycerol (highly viscous Newtonian fluid).

Experimental apparatus II

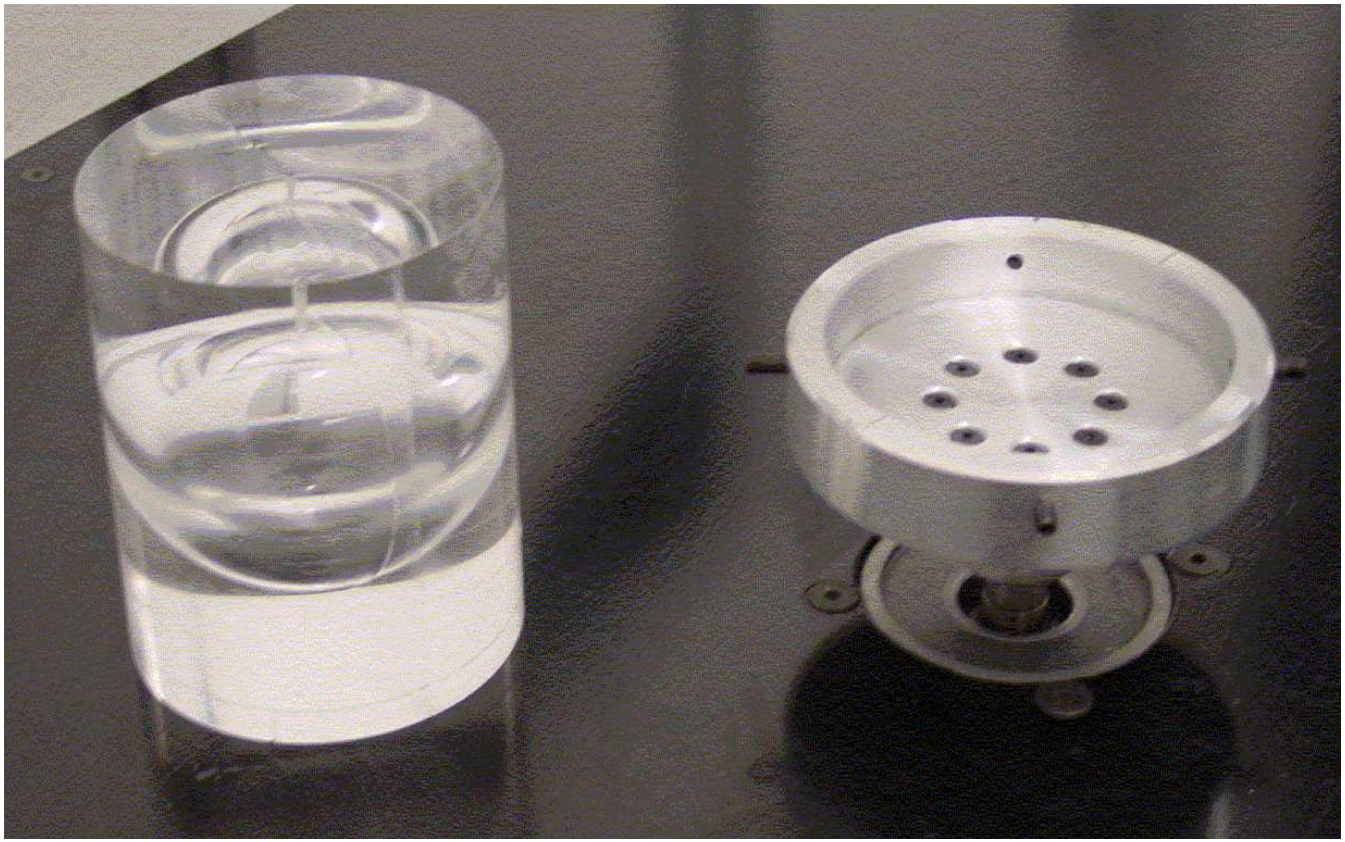

The eye model is mounted on the shaft of a computer controlled motor.

Experimental apparatus III

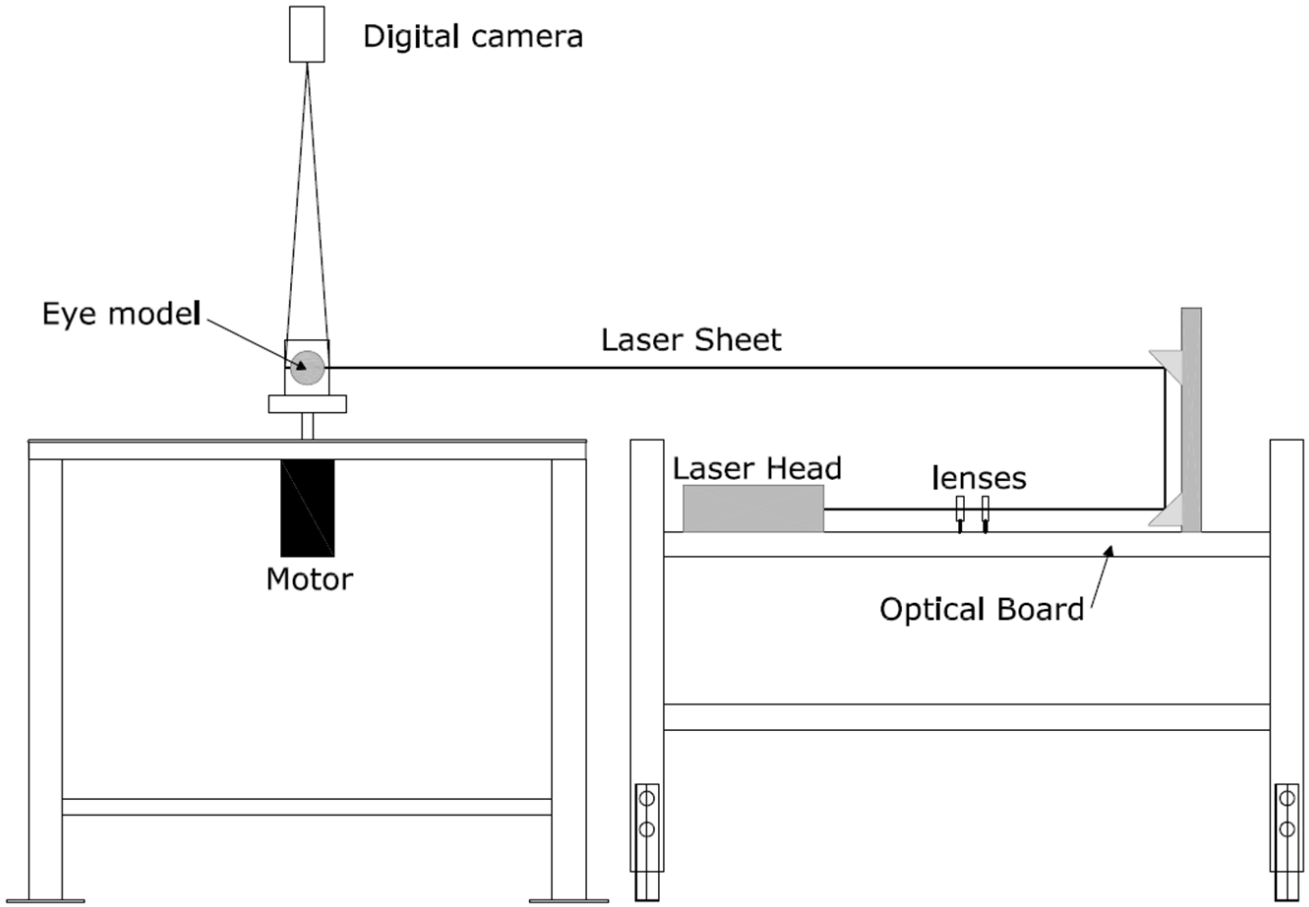

Experimental measurements I

PIV (Particle Image Velocimetry) measurements are taken on the equatorial plane orthogonal to the axis of rotation.

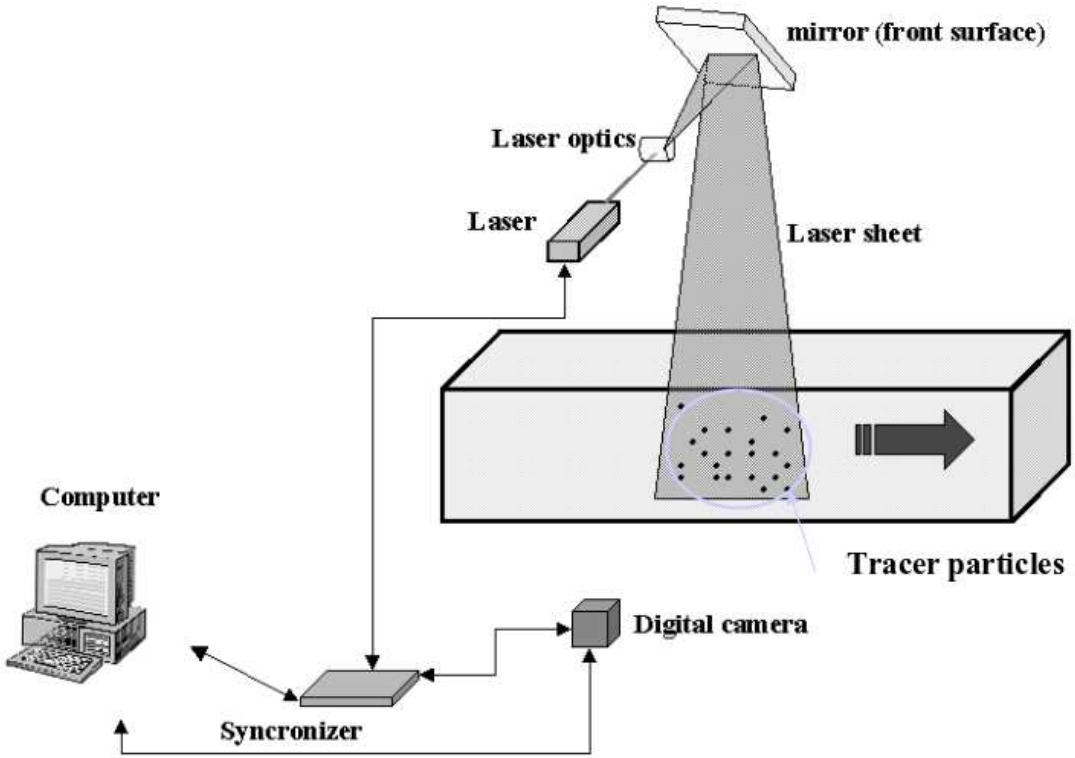

Typical PIV setup

Experimental measurements II

Typical PIV image

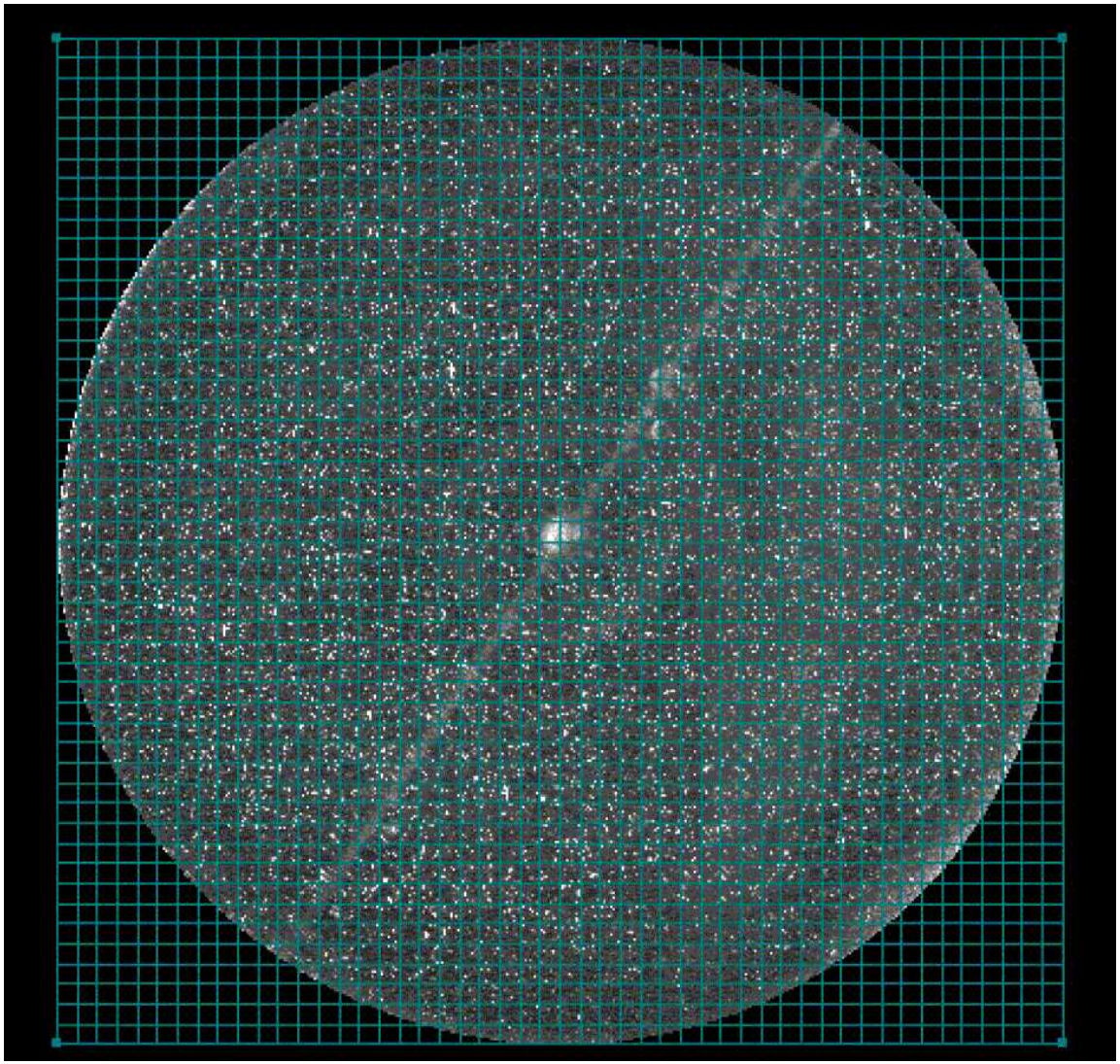

Experimental measurements III

In the PIV technique

- the image is subdivided in small **interrogation windows** (IW);
- **cross-correlation** of the image in each IW at two successive time instants yields the most likely **average displacement** **s** within the IW;
- in each IW the velocity vector is obtained as

$$\mathbf{u} = \frac{\mathbf{s}}{\Delta t},$$

with Δt time step between the two images.

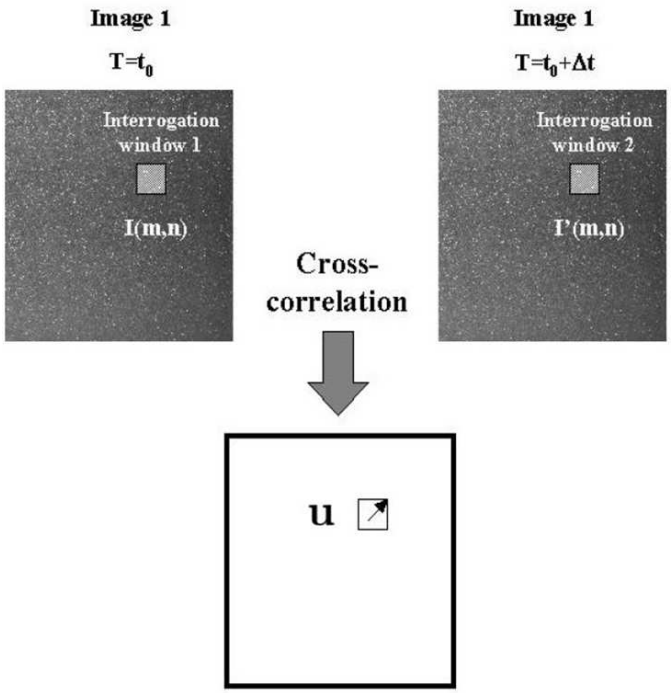

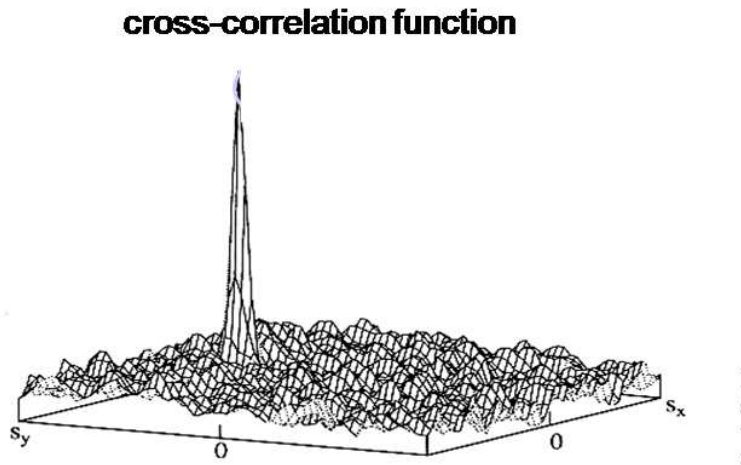

Experimental measurements IV

Typical PIV flow field

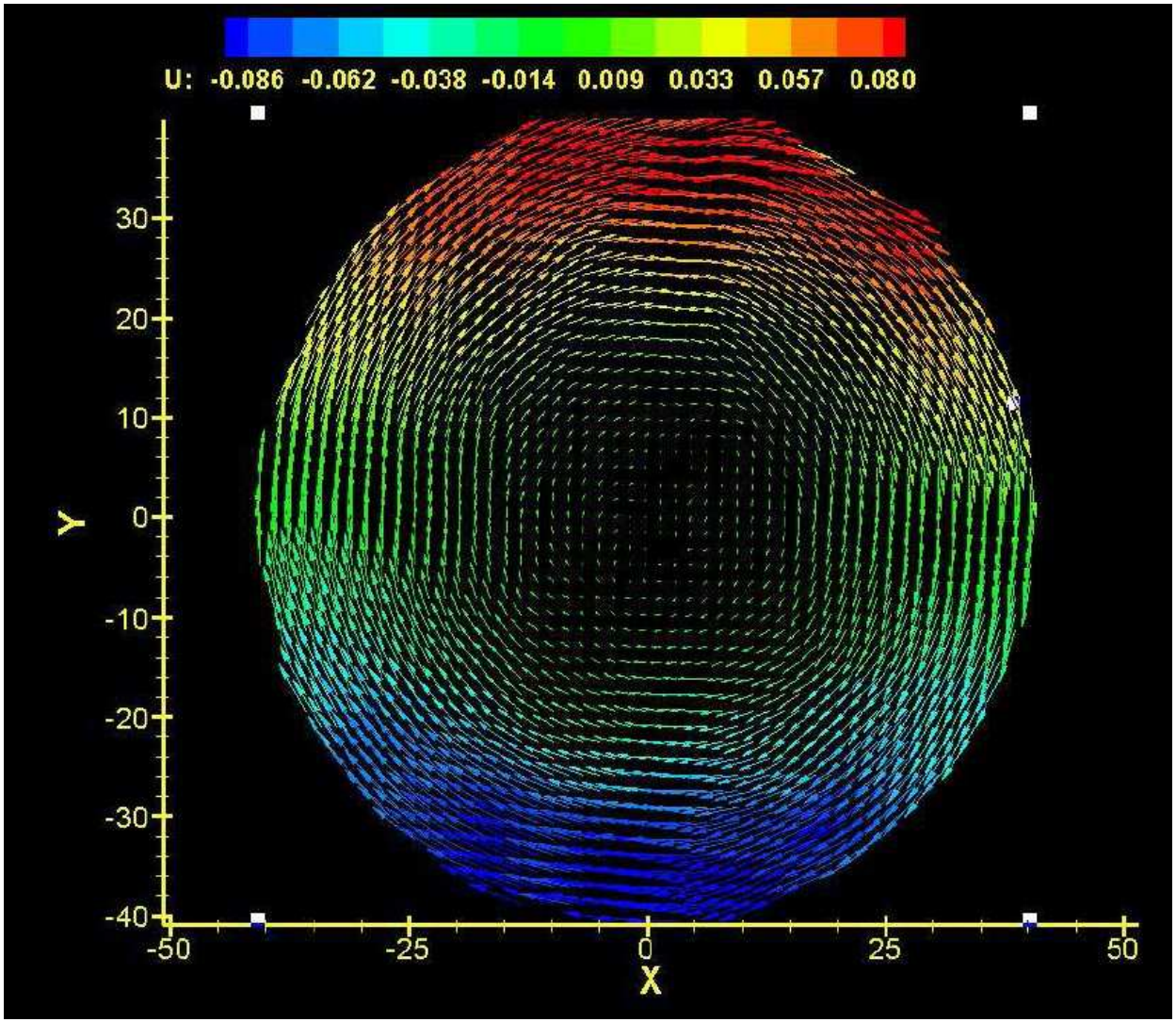

Comparison between experimental and theoretical results

Radial profiles of $\Re(g_1)$, $\Im(g_1)$ and $|g_1|$ for two values of the Womersley number α.

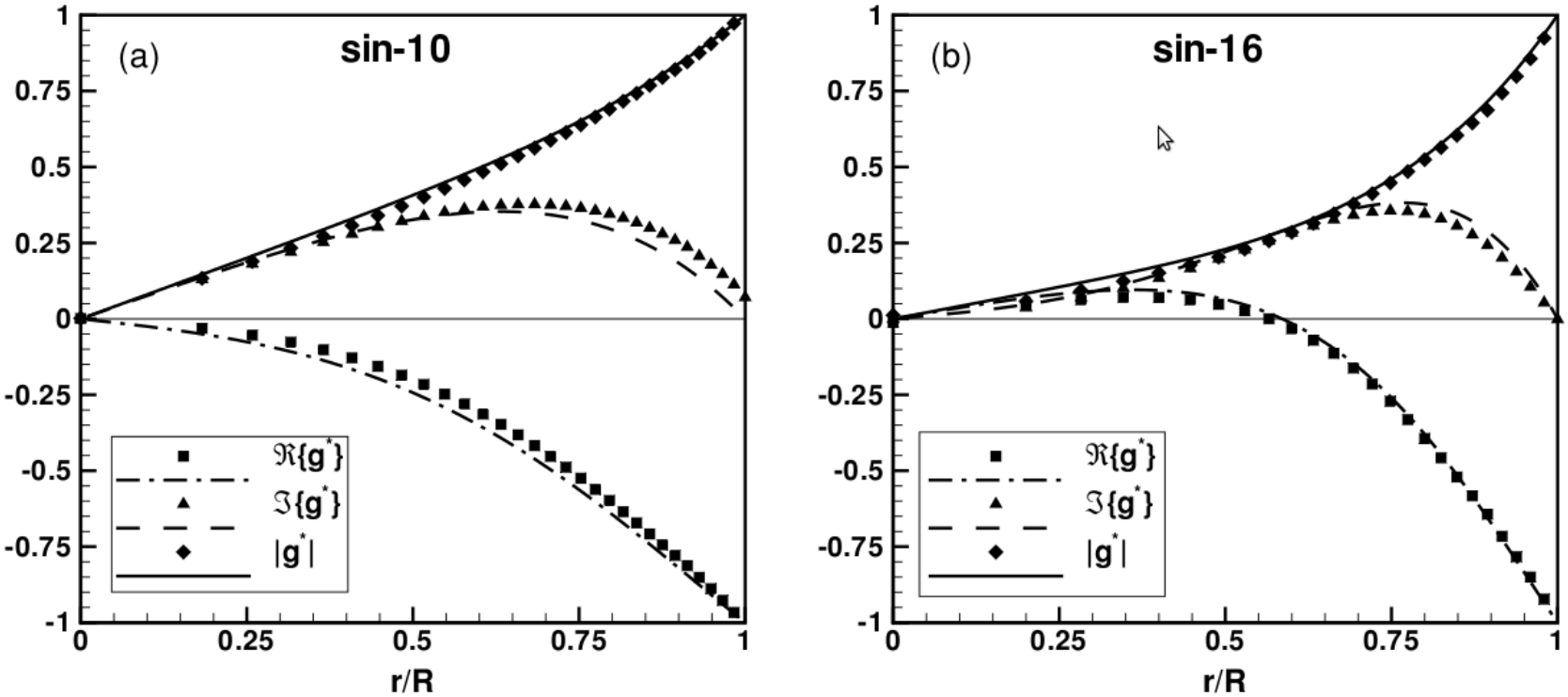

The case of a viscoelastic fluid I

- As we deal with an sinusoidally oscillating linear flow we can obtain the solution for the motion of a viscoelastic fluid simply by replacing the real viscosity with a **complex viscosity.**
- In terms of our dimensionless solution this implies introducing a **complex Womersley number.**
- Rheological properties of the vitreous (complex viscosity) can be obtained from the works of Lee et al. (1992), Nickerson et al. (2008) and Swindle et al. (2008).
- It can be proved that in this case, due to the presence of an elastic component of vitreous behaviour, the system admits natural frequencies that can be excited resonantly by eye rotations.

Formulation of the problem I

The motion of the fluid is governed by the momentum equation and the continuity equation:

$$\frac{\partial \mathbf{u}}{\partial t} + (\mathbf{u} \cdot \nabla)\mathbf{u} + \frac{1}{\rho}\nabla p - \frac{1}{\rho}\nabla \cdot \mathbf{d} = 0, \tag{10a}$$

$$\nabla \cdot \mathbf{u} = 0, \tag{10b}$$

where $\mathbf{d}$ is the deviatoric part of the stress tensor.

Assumptions

- We assume that the velocity is small so that nonlinear terms in (10a) are negligible.
- For a linear viscoelastic fluid we can write

$$\mathbf{d}(t) = 2\int_{-\infty}^{t} G(t-\tilde{t})\mathbf{D}(\tilde{t})d\tilde{t} \tag{11}$$

  where $\mathbf{D}$ is the rate of deformation tensor and G is the relaxation modulus.

Therefore we need to solve the following problem

$$\rho\frac{\partial \mathbf{u}}{\partial t} + \nabla p - \int_{-\infty}^{t} G(t-\tilde{t})\nabla^2\mathbf{u}\, d\tilde{t} = 0, \tag{12a}$$

$$\nabla \cdot \mathbf{u} = 0, \tag{12b}$$

Relaxation behaviour I

We assume that the solution has the structure

$$\mathbf{u}(\mathbf{x}, t) = \mathbf{u}_\lambda(\mathbf{x})e^{\lambda t} + c.c., \qquad p(\mathbf{x}, t) = p_\lambda(\mathbf{x})e^{\lambda t} + c.c.,$$

where $\mathbf{u}_\lambda, p_\lambda$ do not depend on time and $\lambda \in \mathbb{C}$.
It can be shown that the deviatoric part of the stress tensor takes the form

$$\mathbf{d}(t) = 2\int_{-\infty}^{t} G(t-\tilde{t})\mathbf{D}(\tilde{t})d\tilde{t} = 2\mathbf{D}\frac{\tilde{G}(\lambda)}{\lambda}, \tag{13}$$

where

$$\tilde{G}(\lambda) = G'(\lambda) + iG''(\lambda) = \lambda\int_0^\infty G(s)e^{-\lambda s}ds$$

is the complex modulus.

- G': **storage modulus;**
- G'': **loss modulus;**

This leads to the eigenvalue problem

$$\rho\lambda\mathbf{u}_\lambda = -\nabla p_\lambda + \frac{\tilde{G}(\lambda)}{\lambda}\nabla^2\mathbf{u}_\lambda, \quad \nabla\cdot\mathbf{u}_\lambda = 0, \tag{14}$$

which has to be solved imposing **stationary no-slip conditions** at the wall and **regularity conditions** at the origin.

Relaxation behaviour II

Expansion

We expand $(\mathbf{u}_\lambda, p_\lambda)$ in terms of vector spherical harmonics

$$\mathbf{u}_\lambda = \sum_{n=0}^{\infty} \sum_{m=-n}^{n} u_{mn}(r;\lambda)\mathbb{P}_{mn}(\theta,\phi) + v_{mn}(r;\lambda)\mathbb{B}_{mn}(\theta,\phi) + w_{mn}(r;\lambda)\mathbb{C}_{mn}(\theta,\phi), \tag{15a}$$

$$p_\lambda = \sum_{n=0}^{\infty} \sum_{m=-n}^{n} p_{mn}(r;\lambda)\, Y_{mn}(\theta,\phi). \tag{15b}$$

- The vectors $\mathbb{P}_{mn}$ are radial;
- The vectors $\mathbb{B}_{mn}$ and $\mathbb{C}_{mn}$ span the tangential directions with respect to the surface of the unit sphere;
- The vectors $\mathbb{B}_{0n}$ and $\mathbb{C}_{0n}$ are zenithal and azimuthal, respectively;
- The vector spherical harmonics satisfy orthogonality conditions.

Relaxation behaviour III

Solution

Substituting the expansions (15a) and (15b) into (14), equation (14) can be solved and the general solution reads

$$p_{mn} = -\frac{C^{(1)}_{mn}\lambda}{n} r^n, \tag{16a}$$

$$u_{mn} = C^{(1)}_{mn} r^{n-1} + C^{(2)}_{mn} \frac{J_{n+1/2}(ar)}{r^{\frac{3}{2}}}, \tag{16b}$$

$$v_{mn} = \frac{C^{(1)}_{mn} s_n}{n} r^{n-1} + C^{(2)}_{mn} \frac{arJ_{n-1/2}(ar) - nJ_{n+1/2}(ar)}{s_n r^{\frac{3}{2}}}, \tag{16c}$$

$$w_{mn} = C^{(3)}_{mn} \frac{J_{n+1/2}(ar)}{r^{\frac{1}{2}}}, \tag{16d}$$

where J_n is the nth Bessel function of first kind, $s_n = \sqrt{n(n+1)}$, $a = \sqrt{-\rho\lambda^2 R_0^2/\tilde{G}(\lambda)}$ and $C^{(1)}_{mn}$, $C^{(2)}_{mn}$ and $C^{(3)}_{mn}$ are constants to be determined from the boundary conditions.

Relaxation behaviour IV

Enforcing no-slip boundary conditions on the solution (20a)-(20d) and looking for a non trivial solution leads to the condition

$$J_{n+3/2}(a) = 0 \quad \text{or} \quad J_{n+1/2}(a) = 0. \tag{17a, b}$$

We denote the lth positive root of equation (17a) by $a_{ln}^{(1)}$ and the lth positive root of equation (17b) by $a_{ln}^{(2)}$.

The complete **set of eigenfunctions** $(\mathbf{u}_{lmn}^{(k)}, p_{lmn}^{(k)})$, for $k \in \{1, 2\}$, $l \in \mathbb{N}$, $n \in \mathbb{N}_0$, $m \in \mathbb{Z}$, $-n \leq m \leq n$ is given by:

$$\begin{aligned}
\mathbf{u}_{lmn}^{(1)} &= \left(\frac{j_n(a_{ln}^{(1)} r)}{r j_n(a_{ln}^{(1)})} - r^{n-1}\right)\mathbb{P}_{mn} \\
&\quad + \left(\frac{a_{ln}^{(1)} r j_{n-1}(a_{ln}^{(1)} r) - n j_n(a_{ln}^{(1)} r)}{s_n r j_n(a_{ln}^{(1)})} - \frac{n+1}{s_n} r^{n-1}\right)\mathbb{B}_{mn}, \\
p_{lmn}^{(1)} &= \frac{\lambda}{n} r^n Y_{mn}, \\
\mathbf{u}_{lmn}^{(2)} &= j_n(a_{ln}^{(2)} r)\mathbb{C}_{mn}, \\
p_{lmn}^{(2)} &= 0.
\end{aligned}$$

Relaxation behaviour V

Meskauskas et al. (2011) *J. Fluid Mech.*

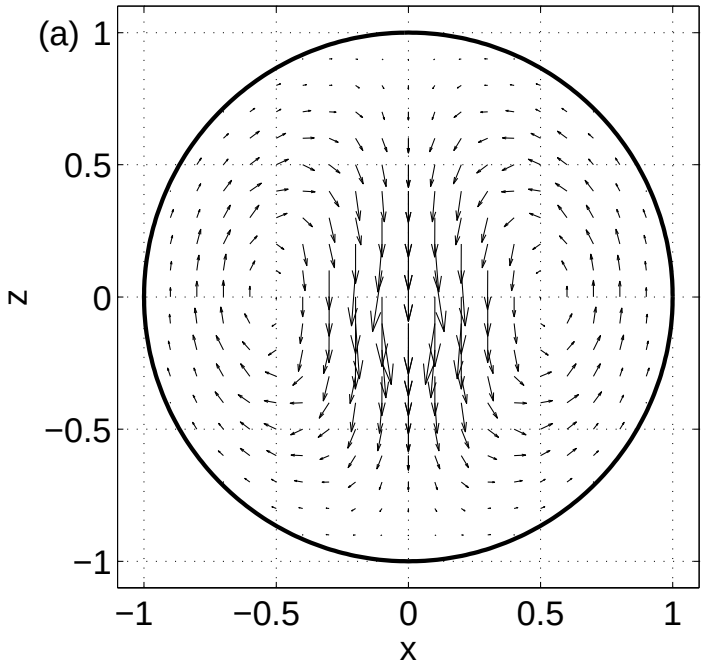

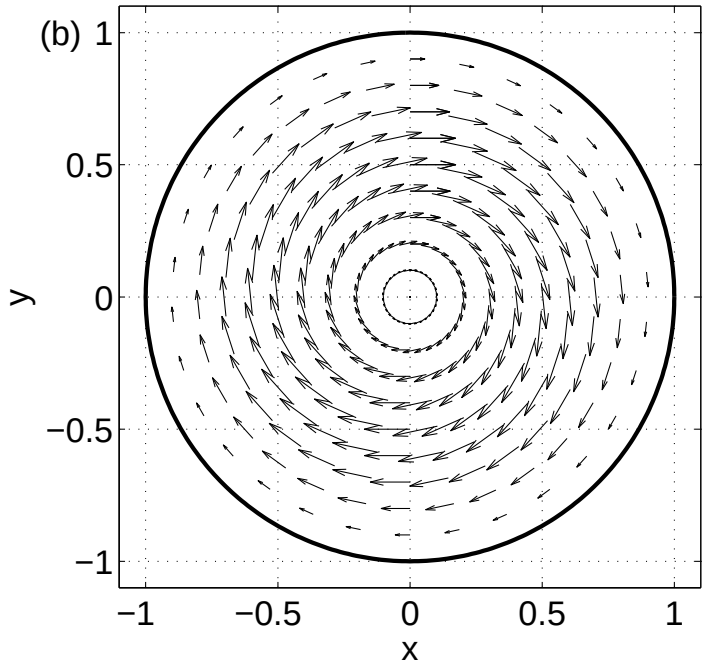

Spatial structure of the eigenfunctions $\mathbf{u}^{(1)}_{102}$ and $\mathbf{u}^{(2)}_{101}$.

Relaxation behaviour VI

The corresponding **eigenvalues** $\lambda_{ln}^{(k)}$ are given by solutions of

$$\lambda_{ln}^{(k)} = \sqrt{-\frac{\tilde{G}(\lambda_{ln}^{(k)})}{\rho R_0^2} a_{ln}^{(k)}}, \tag{18}$$

and depend on how we model the complex modulus $\tilde{G}$.

Two-parameter model

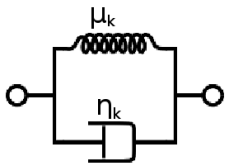

- dashpot: ideal viscous element
- spring: ideal elastic element

$$\tilde{G}(\lambda) = \mu_K + \lambda\eta_K \quad \Rightarrow \quad \lambda_{ln}^{(k)} = -\frac{\eta_K a_{ln}^{(k)2}}{2\rho R_0^2} \pm \sqrt{\frac{\eta_K^2 a_{ln}^{(k)4}}{4\rho^2 R_0^4} - \frac{\mu_K a_{ln}^{(k)2}}{\rho R_0^2}}.$$

Four-parameter model

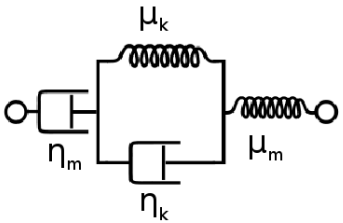

$$\tilde{G}(\lambda) = \frac{\lambda\eta_m\mu_m(\mu_K + \lambda\eta_K)}{(\mu_m + \lambda\eta_m)(\lambda\eta_m\mu_m/(\mu_m + \lambda\eta_m) + \mu_K + \lambda\eta_K)}$$

Some conclusions

- For all existing measurements of the rheological properties of the vitreous we find the **existence of natural frequencies of oscillation.**
- Such frequencies, for the least decaying modes, are within the range of physiological eye rotations ($\omega = 10 - 30$ rad/s).
- The two- and the four-parameter model lead to qualitatively different results:
  - **Two-parameter model:** only a finite number of modes have complex eigenvalues;
  - **Four-parameter model:** an infinite number of modes have complex eigenvalues.
- **Natural frequencies could be resonantly excited by eye rotations.**

Periodic forcing I

Solution

- Response to eye rotations: forced small amplitude sinusoidal torsional oscillations of an angular frequency ω_0.
- Now the boundary condition reads

$$\mathbf{u} = \epsilon\omega_0 R_0 \sin\theta \sin(\omega_0 t)\mathbf{e}_\varphi$$

- The solution is then given by

$$\mathbf{u} = \sqrt{\frac{\pi}{3}} \frac{\epsilon R_0 \omega_0 J_{3/2}(ar)}{iJ_{3/2}(a)\sqrt{r}} e^{i\omega_0 t}\mathbb{C}_{01} + \text{c.c.}$$

The velocity field is **purely azimuthal.**

Periodic forcing II

Normalised kinetic energy

We consider the time-average of the kinetic energy over a cycle

$$\overline{\mathcal{K}} = \frac{2\pi}{3}\rho R_0^5 \omega_0^2 \epsilon^2 \int_0^1 |\frac{J_{3/2}(ar)}{J_{3/2}(a)\sqrt{r}}|^2 r^2 dr,$$

and normalise it with the kinetic energy of a rigid sphere with the same density $(2/15\pi\rho R^5\omega_0^2\epsilon^2)$.

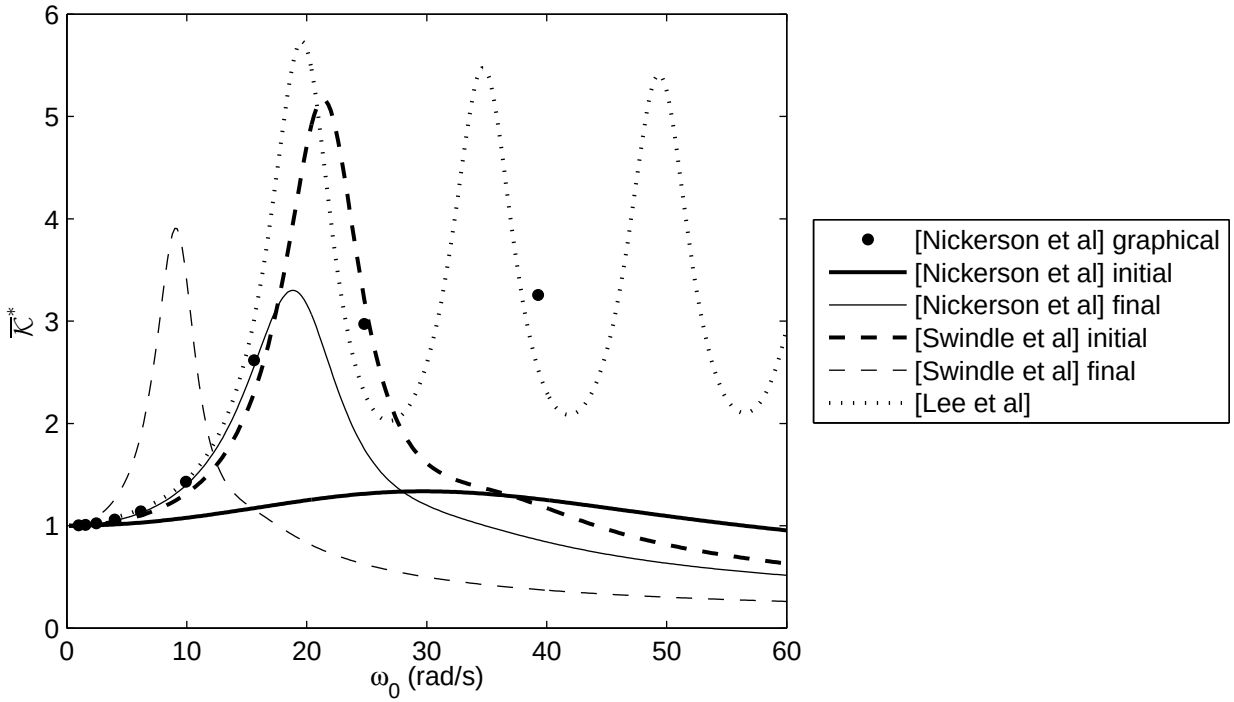

Normalised kinetic energy vs the oscillation frequency.

Periodic forcing III

Velocity profiles

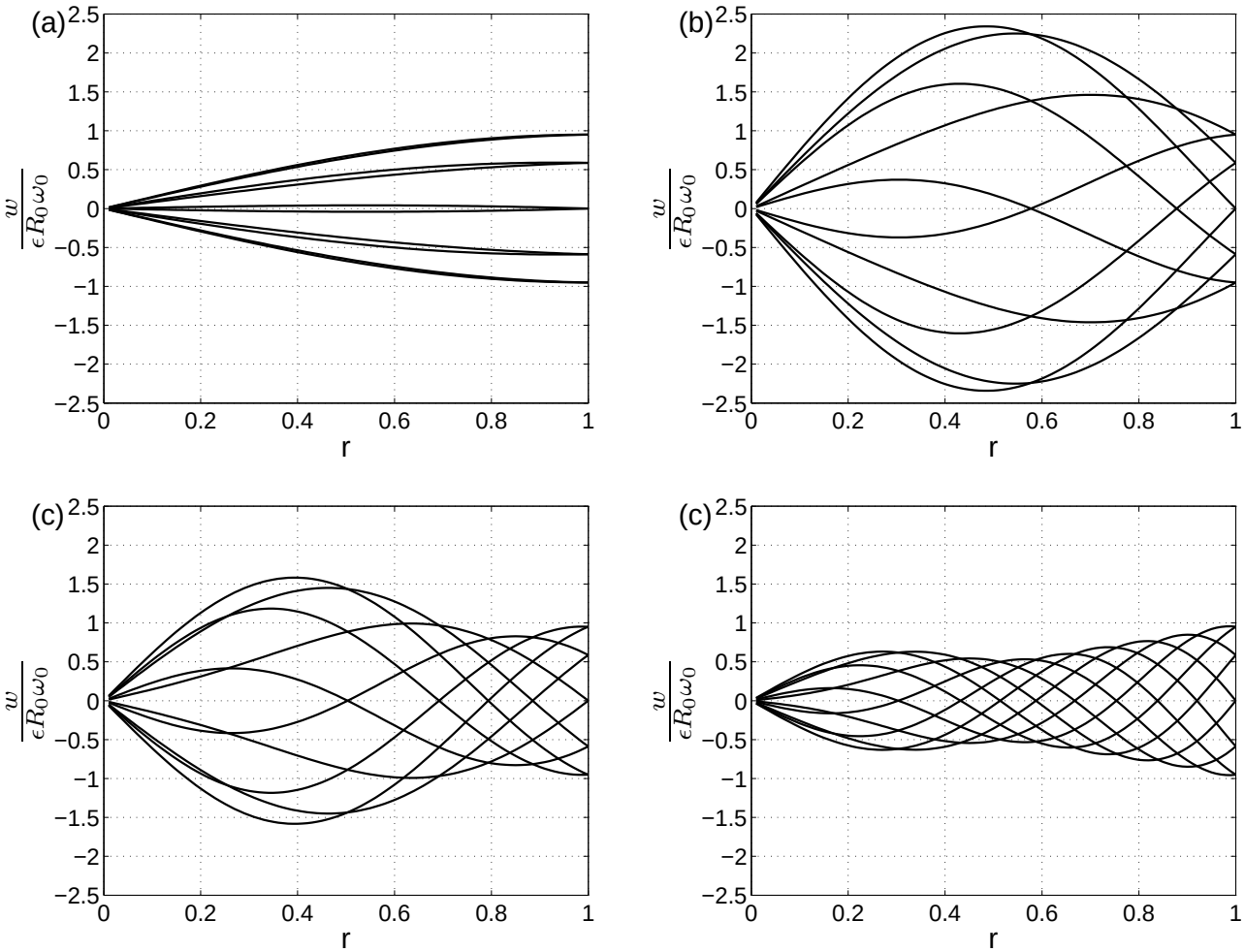

Azimuthal velocity profiles, (a) $\omega = 10$, (b) $\omega = 19.1494$, (c) $\omega = 28$, and (d) $\omega = 45$.

Periodic forcing IV

Shear stress at the wall

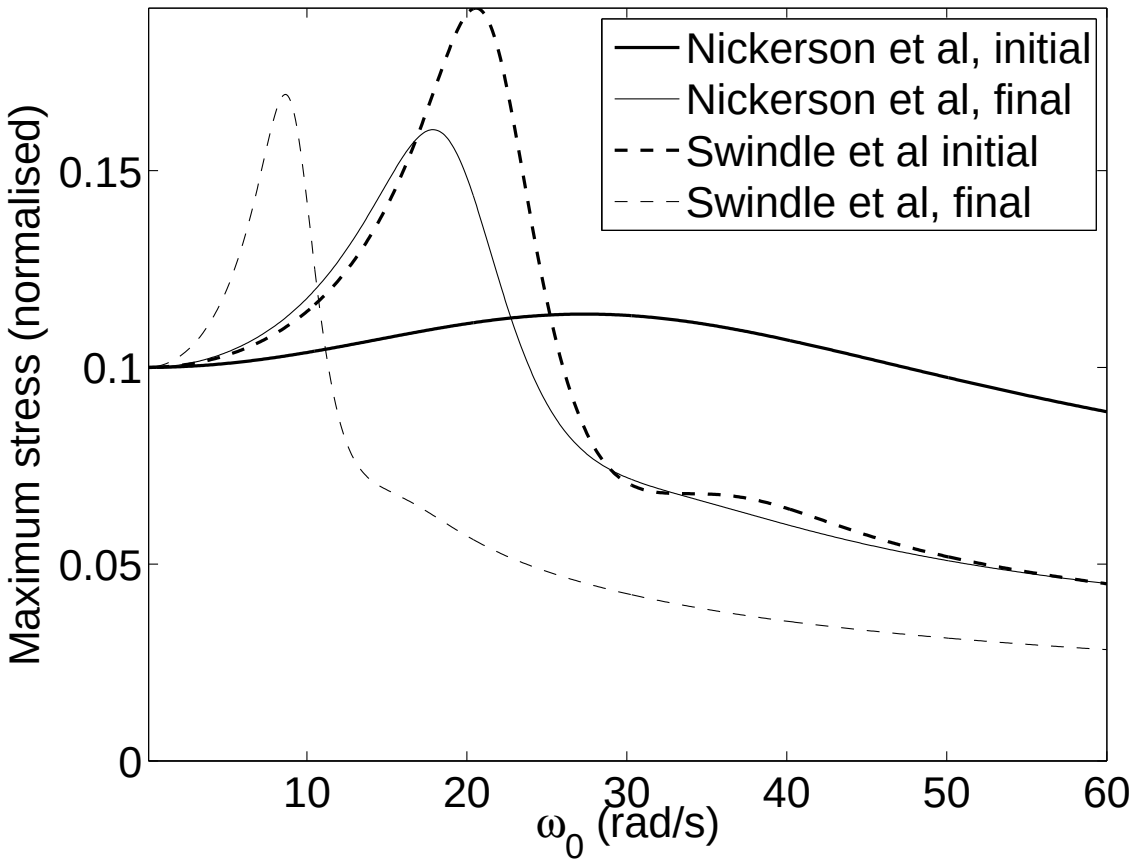

Stress normalised with $\epsilon\rho R^2\omega_0^2$ vs the oscillation frequency.

Some conclusions

- If the eye rotates at certain frequencies resonant excitation is possible.
- Resonance leads to large values of the stress on the retina.
- Does resonant excitation really occurs in-vivo?
  - Need for in-vivo measurements of vitreous velocity (**Ultrasound scan of vitreous motion**).

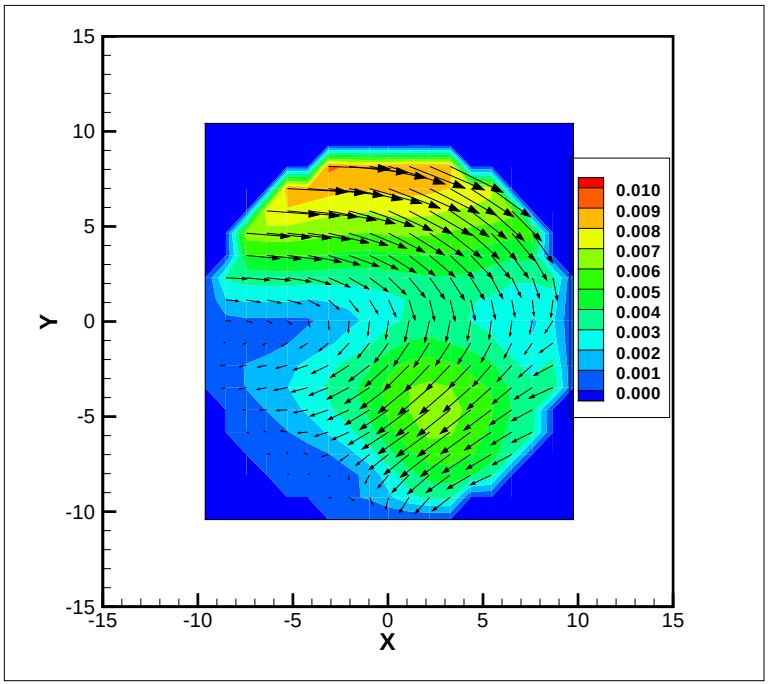

Echo-PIV measurement of vitreous motion (in collaboration with T. Rossi, A. Stocchino, G. Querzoli)

  - Are ev-vivo measurements of vitreous rheological properties reliable?
- The possible occurrence of resonance has implications for the choice of tamponade fluids to be used after vitrectomy.

The effect of the geometry I

- **Myopic eyes;**
- **eye subjects to scleral buckling.**

Myopic Eyes

In comparison to emmetropic eyes, myopic eyes are

- larger in all directions;
- particularly so in the antero-posterior direction.

Myopic eyes bear **higher risks of posterior vitreous detachment and vitreous degeneration** $\rightarrow$ increased the risk of rhegmatogeneous retinal detachment.

The shape of the eye ball has been related to the degree of myopia (measured in dioptres D) by Atchison et al. (2005), who approximated the vitreous chamber with an ellipsoid.

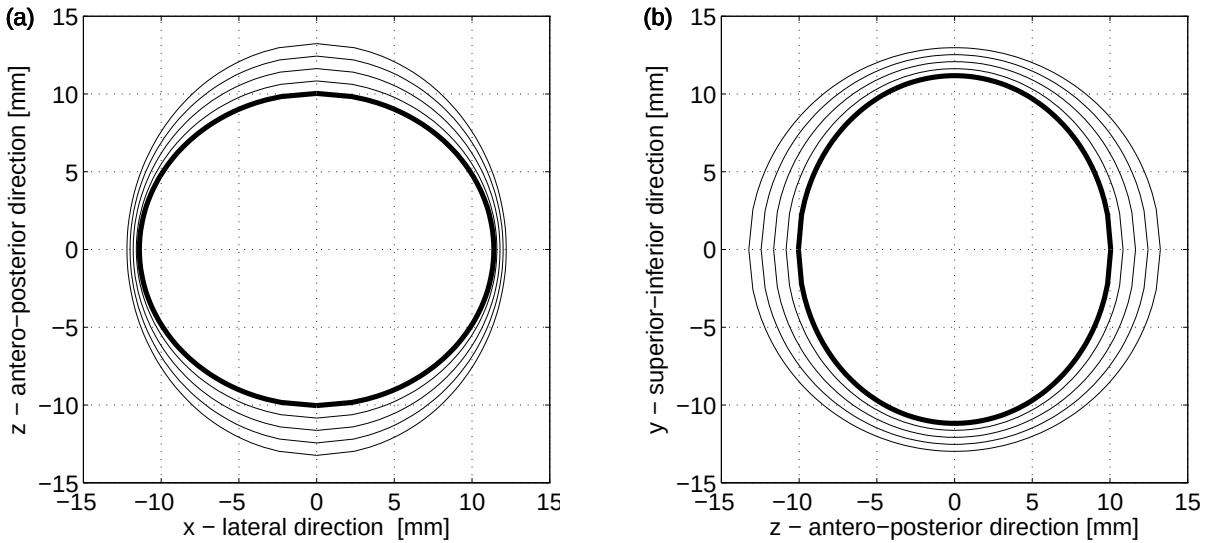

$$\text{width} = 11.4 - 0.04D,$$
$$\text{height} = 11.18 - 0.09D,$$
$$\text{length} = 10.04 - 0.16D.$$

(a) horizontal and (b) vertical cross sections of the domain for different degrees of

The effect of the geometry II

Scleral Buckling

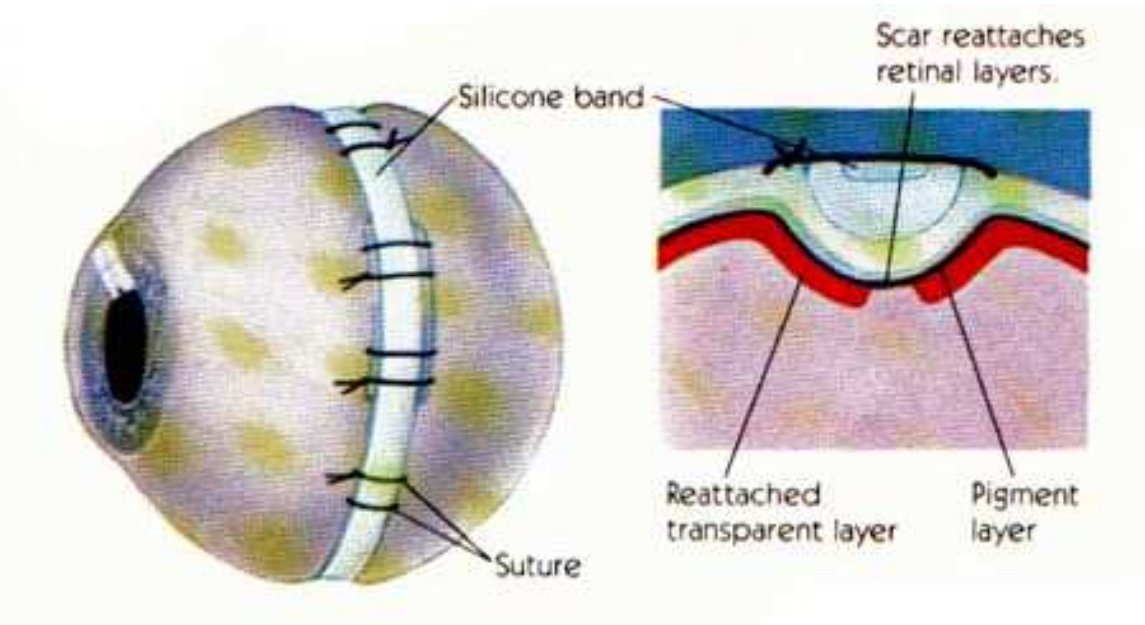

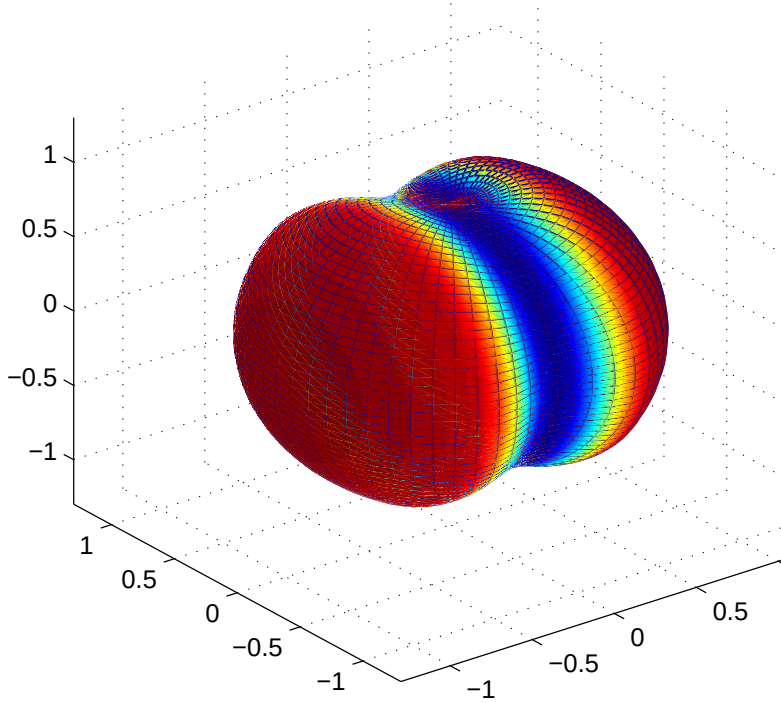

Formulation of the mathematical problem

Meskauskas et al., submitted to Invest. Ophthal. Vis. Scie.

Equation of the boundary

$$R(\vartheta, \varphi) = R_0(1 + \delta R_1(\vartheta, \varphi)),$$

where

- R_0 denotes the radius of the sphere with the same volume as the vitreous chamber;
- δ is a **small parameter** ($\delta \ll 1$);
- the maximum absolute value of R_1 is 1.

Expansion

We expand the velocity and pressure fields in therms of δ as follows

$$\mathbf{U} = \mathbf{U}_0 + \delta \mathbf{U}_1 + \mathcal{O}\left(\delta^2\right), \qquad P = P_0 + \delta P_1 + \mathcal{O}\left(\delta^2\right).$$

Solution I

Leading order problem $\mathcal{O}(\delta^0)$

At leading order we find the solution in a sphere, discussed above.

Order δ problem

At leading order we find the solution in a sphere, discussed above.
To compute the solution at δ-order, we expand $\mathbf{U}_1$, P_1 as a sum of spherical harmonics

$$\mathbf{U}_1 = \Bigg(\sum_{n=0}^{\infty} \sum_{m=-n}^{n} \mathcal{U}_1^{mn}(r)\mathbb{P}_{mn}(\vartheta,\varphi) + \mathcal{V}_1^{mn}(r)\mathbb{B}_{mn}(\vartheta,\varphi) + \mathcal{W}_1^{mn}(r)\mathbb{C}_{mn}(\vartheta,\varphi) \Bigg) e^{i\omega t} + c.c.$$

$$P_1 = \sum_{n=0}^{\infty} \sum_{m=-n}^{n} P_1^{mn}(r) Y_{mn}(\vartheta,\varphi) e^{i\omega t} + c.c.$$

Solution II

Scaling

We work in terms of the following dimensionless variables

$$r = \frac{r^*}{R_0}, \quad t = t^*\omega, \quad \mathbf{U} = \frac{\mathbf{U}^*}{\omega R_0}, \quad P = \frac{P^*}{\rho\omega^2 R_0^2}, \quad \sigma = \frac{\sigma^*}{\rho\omega^2 R_0^2}. \qquad (19a-e)$$

Boundary conditions at the wall

At δ-order the boundary conditions at $r = 1$ read

$$\begin{aligned}\mathbf{U}_1|_{r=1} =& R_1(\vartheta,\varphi)\left(-\frac{\epsilon i \sin\vartheta}{2} - \left.\frac{\partial W_0}{\partial r}\right|_{r=1}\right)\mathbf{e}_\varphi \\ =& \sum_{n=0}^{\infty}\sum_{m=-n}^{n}\left(\hat{\mathcal{V}}_1^{mn}\mathbb{B}_{mn}(\vartheta,\varphi) + \hat{\mathcal{W}}_1^{mn}\mathbb{C}_{mn}(\vartheta,\varphi)\right),\end{aligned}$$

where $\hat{\mathcal{V}}_1^{mn}$ and $\hat{\mathcal{W}}_1^{mn}$ depend on the shape of the domain.

Solution III

Solution at the order δ

$$P_1^{mn} = -C_1^{mn}\frac{i\alpha_c^2}{n}r^n, \tag{20a}$$

$$\mathcal{U}_1^{mn} = C_1^{mn}r^{n-1} + C_2^{mn}\frac{J_{n+1/2}(ar)}{r^{3/2}}, \tag{20b}$$

$$\mathcal{V}_1^{mn} = C_1^{mn}\frac{s_n}{n}r^{n-1} + \frac{C_2^{mn}}{s_n r^{3/2}}\left(-nJ_{n+1/2}(ar) + arJ_{n-1/2}(ar)\right), \tag{20c}$$

$$\mathcal{W}_1^{mn} = C_3^{mn}\frac{J_{n+1/2}(ar)}{\sqrt{r}}, \tag{20d}$$

for $n > 0$, and $P_1^{00} = \mathcal{U}_1^{00} = 0$, where J_k denotes the Bessel function of order k, $s_n = \sqrt{n(n+1)}$, and the boundary condition at the wall implies

$$C_1^{mn} = \frac{-s_n J_{n+1/2}(a)\hat{\mathcal{V}}_{mn}}{aJ_{n-1/2}(a) - (2n+1)J_{n+1/2}(a)}, \tag{21a}$$

$$C_2^{mn} = \frac{s_n \hat{\mathcal{V}}_{mn}}{aJ_{n-1/2}(a) - (2n+1)J_{n+1/2}(a)}, \tag{21b}$$

$$C_3^{mn} = \frac{\hat{\mathcal{W}}_{mn}}{J_{n+1/2}(a)}. \tag{21c}$$

Solution IV

Stress at the boundary

Order δ^0

$$\mathbf{T}_0|_{r=1} = \frac{1}{\alpha_c^2}\left(\frac{\partial W_0}{\partial r} - \frac{W_0}{r}\right)\Big|_{r=1}\mathbf{e}_\varphi = -\frac{\epsilon i}{2\alpha_c^2}\left(\frac{(a^2-3)\sin a - a\cos a}{\sin a - a\cos a}\right)\sin\vartheta\mathbf{e}_\varphi + c.c..$$

Order δ

$$\begin{aligned}\mathbf{T}_1|_{r=1} = & \left(-P_1 + \frac{1}{\alpha_c^2}\left(2\frac{\partial U_1}{\partial r} - \left(\frac{\partial W_0}{\partial r} - W_0\right)\frac{\partial R_1}{\partial \varphi}\operatorname{cosec}\vartheta\right)\right)\Big|_{r=1}\mathbf{e}_r \\ & + \frac{1}{\alpha_c^2}\left(\frac{\partial V_1}{\partial r} - V_1 + \frac{\partial U_1}{\partial \vartheta}\right)\Big|_{r=1}\mathbf{e}_\vartheta \\ & + \frac{1}{\alpha_c^2}\left(\frac{1}{\sin\vartheta}\frac{\partial U_1}{\partial \varphi} + \frac{\partial W_1}{\partial r} - W_1 + R_1\left(\frac{\partial^2 W_0}{\partial r^2} - \frac{\partial W_0}{\partial r} + W_0\right)\right)\Big|_{r=1}\mathbf{e}_\varphi.\end{aligned}$$

Myopic eyes I

Stress distribution on the retina

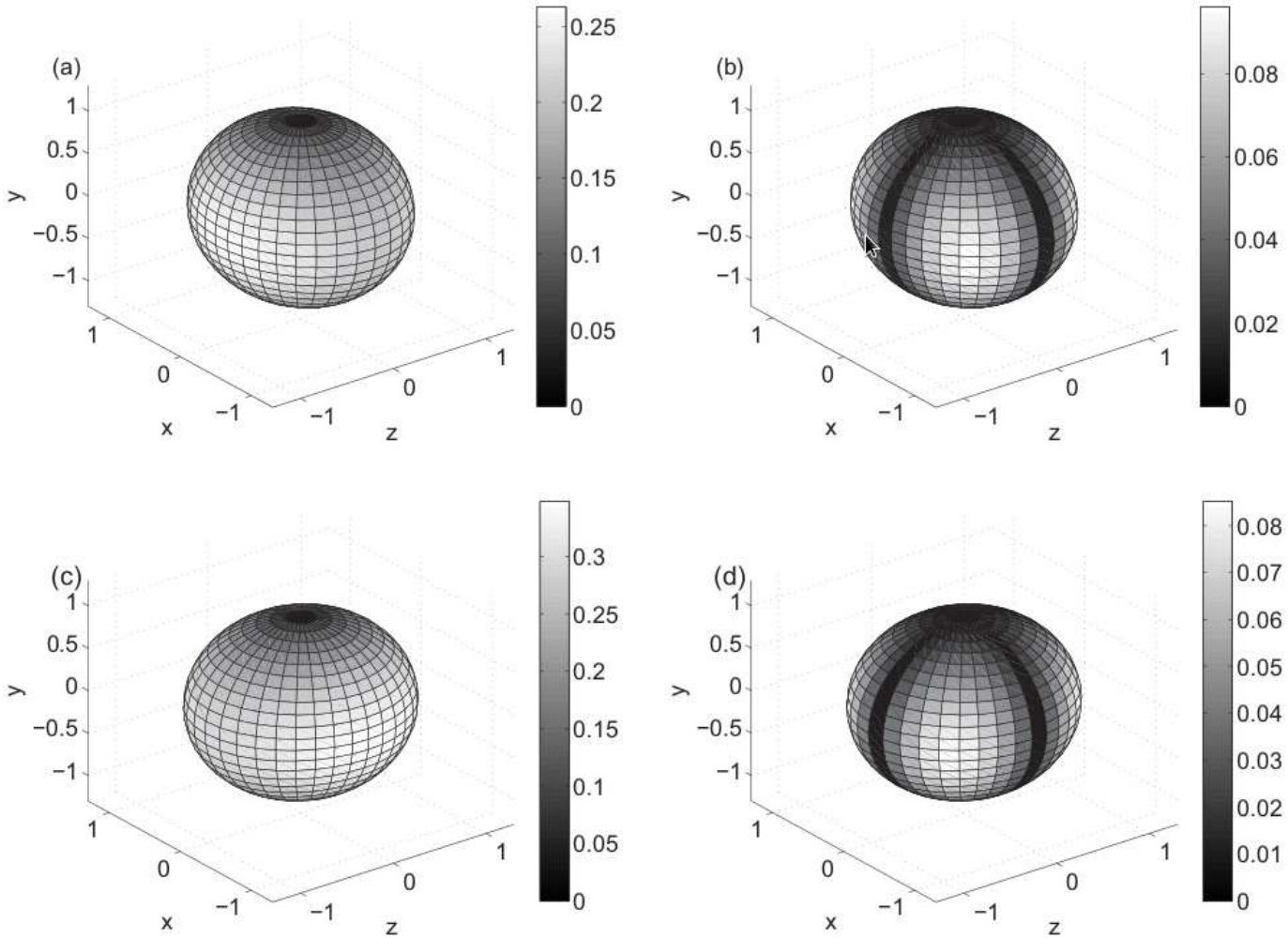

Spatial distribution of (a, c) the maximum dimensionless tangential stress and (b, d) normal stress. (a) and (b): emmetropic eye; (c) and (d): myopic eye with refractive error 20 D.

Myopic eyes II

Maximum stress on the retina as a function of the refractive error

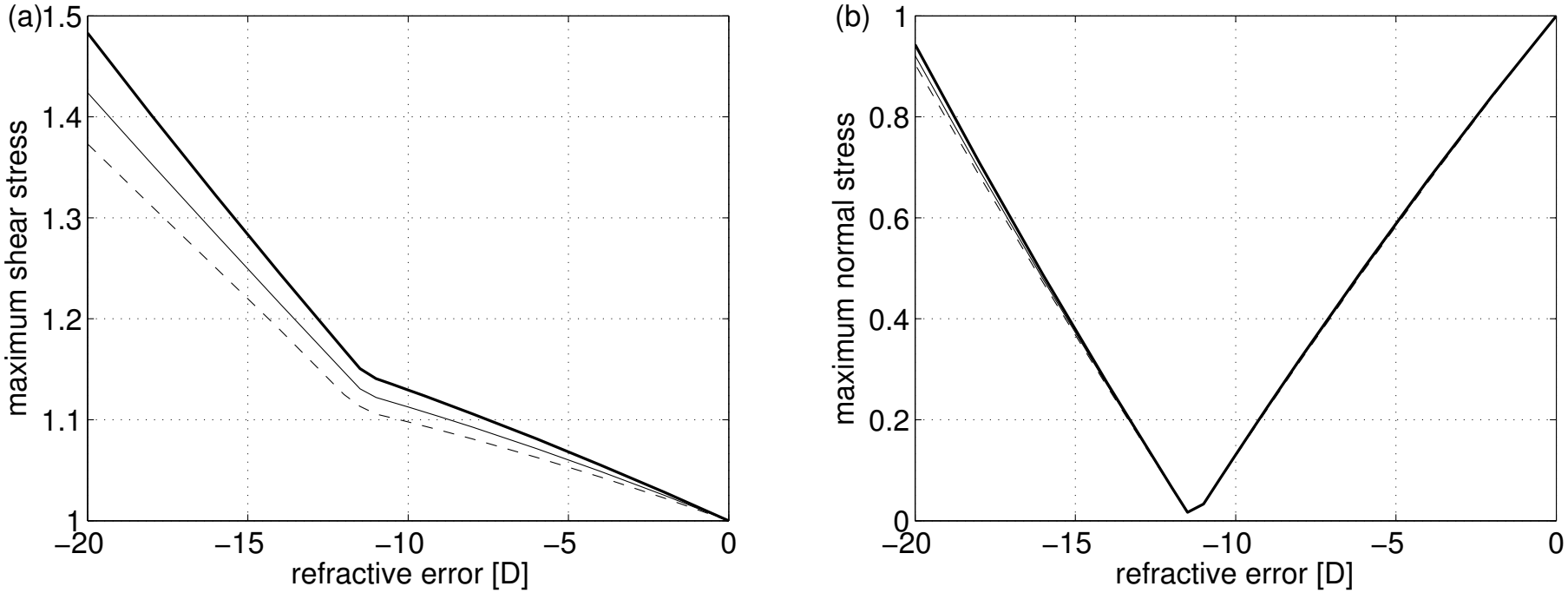

Maximum (over time and space) of the (a) tangential and (b) normal stress on the retina as a function of the refractive error in dioptres. **Values are normalised with the corresponding stress in the emmetropic (0 D) eye.** The different curves correspond to different values of the rheological properties of the vitreous humour taken from the literature.

Scleral buckling I

Stress distribution on the retina

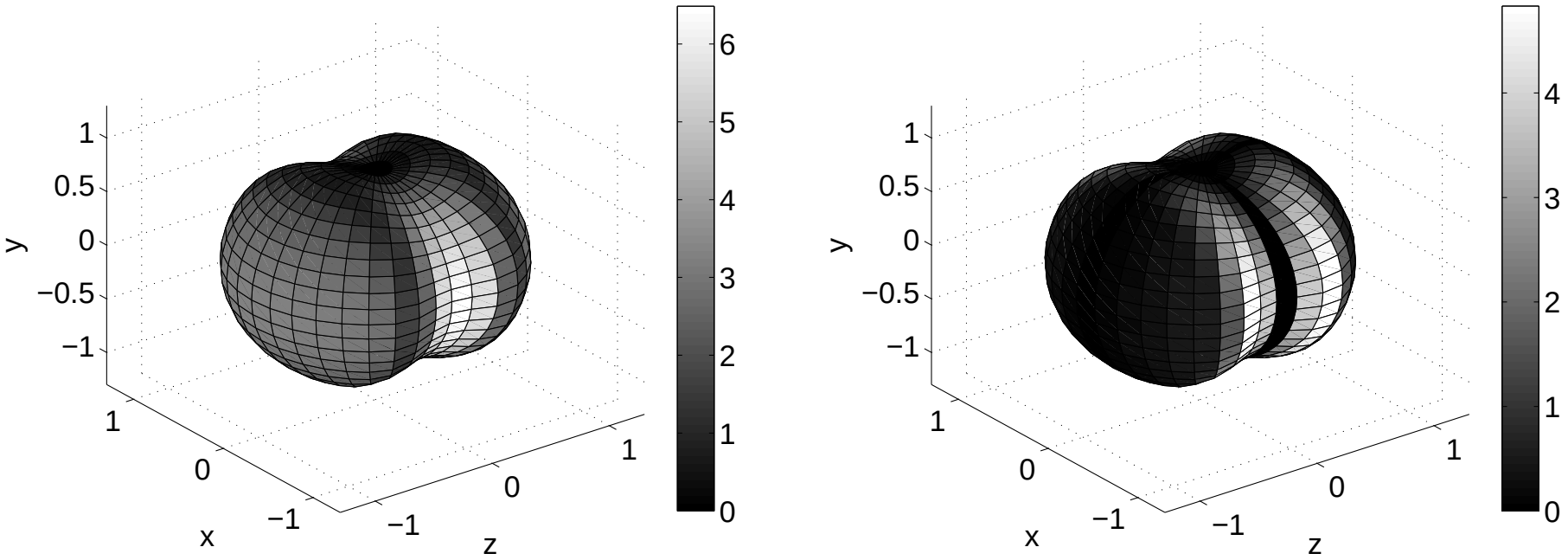

Spatial distribution of the leading+δ-order maximum shear stress (left) and normal stress (right) over time.

Scleral buckling II

Maximum shear stress (a) and normal stress (n) in dependence of the ratio $R_i/\hat{R}$.

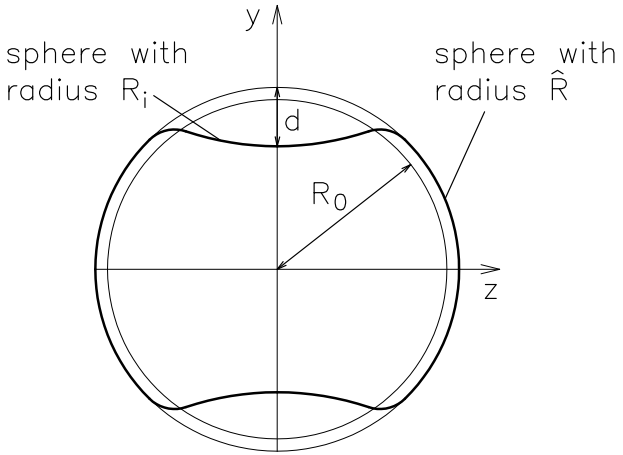

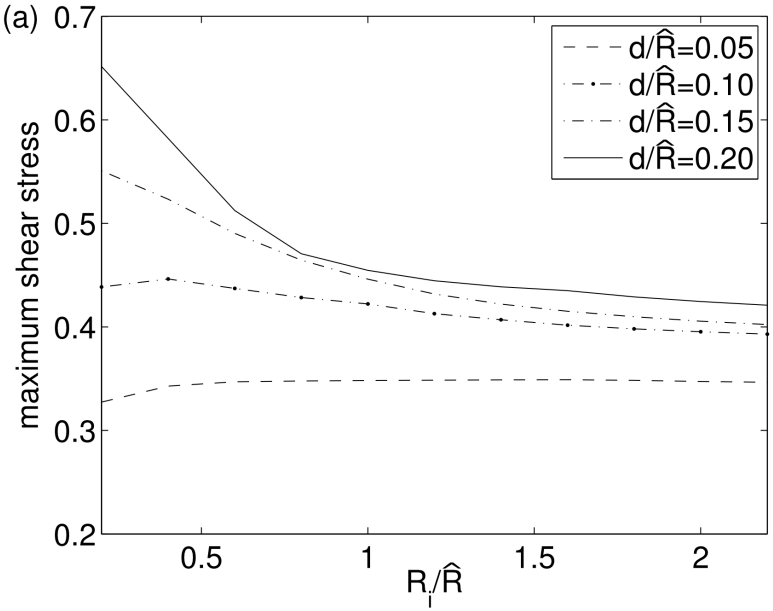

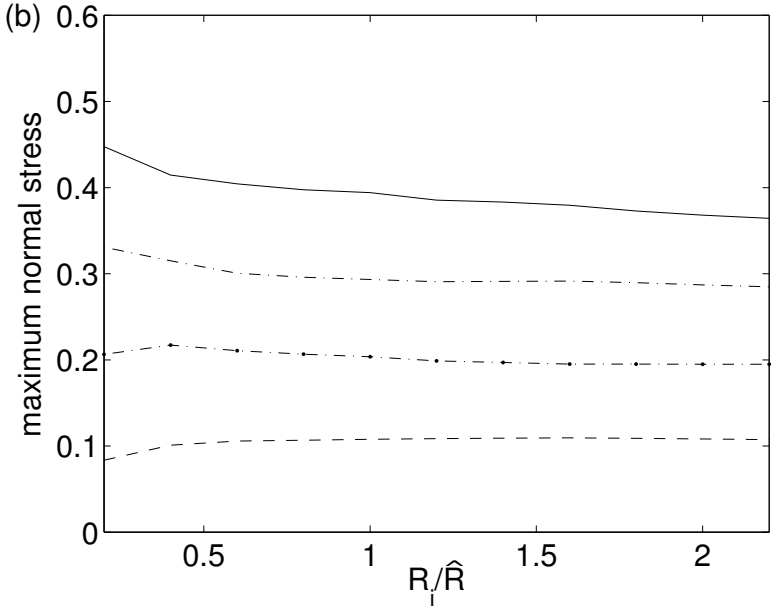

Some conclusions

- The vitreous and the retina in myopic eyes are continuously subjected to **higher shear stresses than emmetropic eyes.**
- This provides a feasible explanation for why in myopic eyes vitreous liquefaction, PVD and RD are more frequent than in emmetropic eyes.

- Scleral buckling induced a significant **change in the stress distribution on the retina.**
- In particular the pressure drop across the detached retinal flap might help reattachment.
- In order to fully understand the mechanics of the reattachment process further models would be required, accounting for the motion of the detached retina and of the fluid in the subretinal space.

Non-linear effects and implications for fluid mixing

Back to viscous fluids . . .

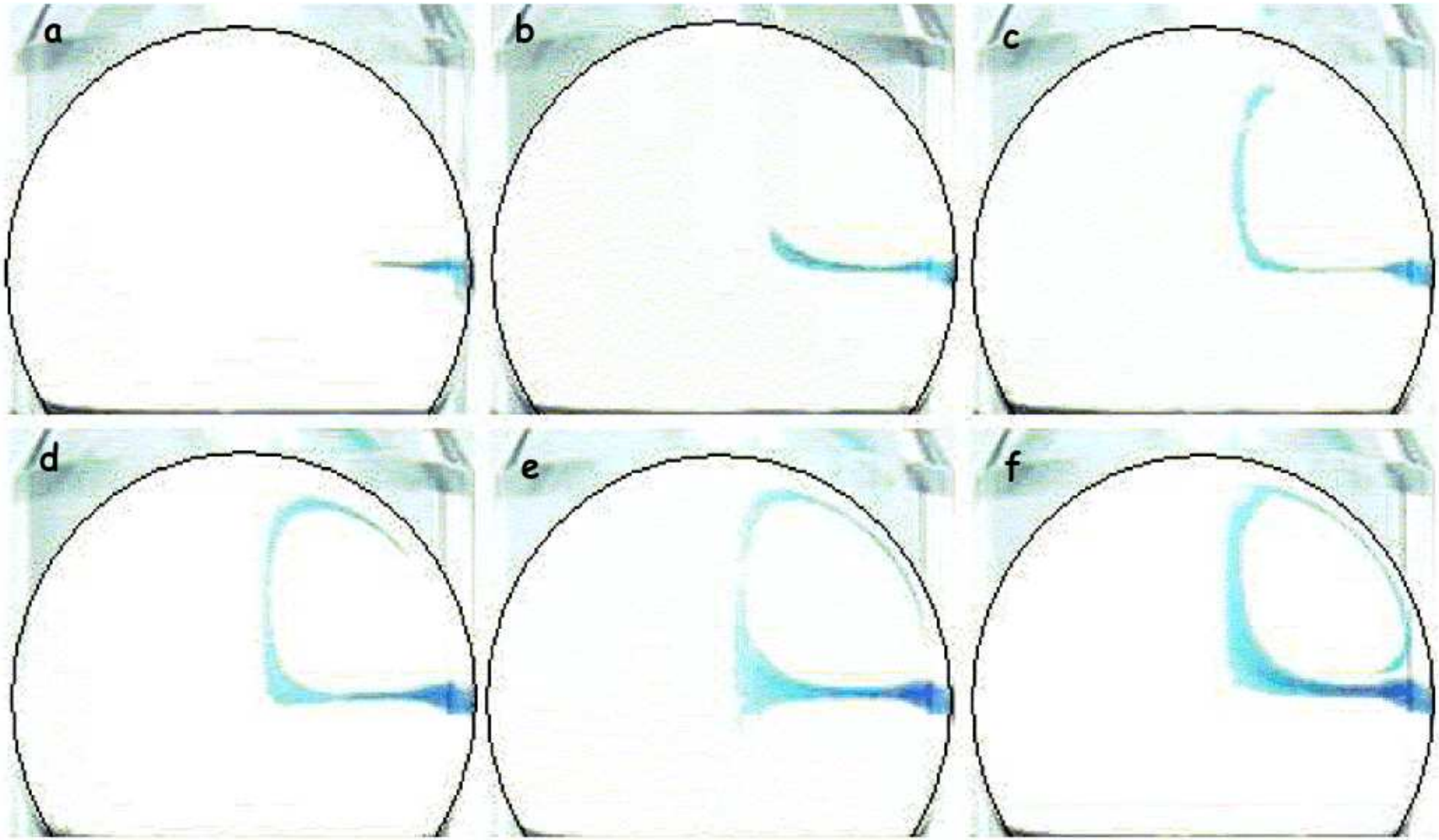

Flow visualisations on planes containing the axis of rotation.

Theoretical model I

Second order solution

$$\mathbf{u} = \varepsilon \mathbf{u}_1 + \varepsilon^2 \mathbf{u}_2 + \mathcal{O}(\varepsilon^3), \quad p = \varepsilon p_1 + \varepsilon^2 p_2 + \mathcal{O}(\varepsilon^3).$$

We decompose the velocity $\mathbf{u}_2$ and the pressure p_2 into their **time harmonics** by setting

$$\mathbf{u}_2 = \mathbf{u}_{20} + \left\{ \mathbf{u}_{22} e^{2it} + c.c. \right\}, \quad p_2 = p_{20} + \left\{ p_{22} e^{2it} + c.c. \right\}, \quad \mathbf{u}_1 \cdot \boldsymbol{\nabla} \mathbf{u}_1 = \mathcal{F}_0 + \left\{ \mathcal{F}_2 e^{2it} + c.c. \right\},$$

where $\mathbf{u}_{20}$, $\mathbf{u}_{22}$, p_{20}, p_{22}, $\mathcal{F}_0$ and $\mathcal{F}_2$ are independent of time.

Governing equations for the steady component

$$\nabla^2 \mathbf{u}_{20} - \boldsymbol{\nabla} p_{20} = \alpha^2 \mathcal{F}_0, \qquad \boldsymbol{\nabla} \cdot \mathbf{u}_{20} = 0, \tag{22a}$$

$$u_{20} = v_{20} = w_{20} = 0 \qquad (r = 1). \tag{22b}$$

Theoretical model II

Expansion in terms of spherical harmonics

Using the orthogonality properties of the vector spherical harmonics it may be shown that

$$\mathcal{F}_0 = \mathcal{F}_{P0}(r)\mathbb{P}_0^0(\vartheta,\varphi) + \mathcal{F}_{P2}(r)\mathbb{P}_2^0(\vartheta,\varphi) + \mathcal{F}_{B2}(r)\mathbb{B}_2^0(\vartheta,\varphi)$$

where

$$\mathcal{F}_{P0} = -\frac{8}{3}\sqrt{\pi}\frac{g_1\overline{g_1}}{r}, \quad \mathcal{F}_{P2} = \frac{8}{15}\sqrt{5\pi}\frac{g_1\overline{g_1}}{r}, \quad \mathcal{F}_{B2} = \frac{4}{15}\sqrt{30\pi}\frac{g_1\overline{g_1}}{r}.$$

Owing to the special behaviour of the vector spherical harmonics under vector calculus, operators $\mathbf{u}_{20} = (u_{20}, v_{20}, w_{20})$ and p_{20} can be expanded as

$$\mathbf{u}_{20} = u_{20,0}(r)\mathbb{P}_0^0(\vartheta,\varphi) + u_{20,2}(r)\mathbb{P}_2^0(\vartheta,\varphi) + v_{20,2}(r)\mathbb{B}_2^0(\vartheta,\varphi), \tag{23a}$$

$$p_{20} = p_{20,0}\,Y_0^0(\vartheta,\varphi) + p_{20,2}\,Y_2^0(\vartheta,\varphi). \tag{23b}$$

Notes:

- the azimuthal velocity component w_{20} vanishes;
- velocity vectors of the steady streaming lie on the planes containing the axis of rotation.

Theoretical model III

By substituting the expansions (23a,b) into equations (22a) the following ordinary differential problem in r is obtained

$$\frac{d^2}{dr^2}u_{20,0} + \frac{2}{r}\frac{d}{dr}u_{20,0} - 2\frac{u_{20,0}}{r^2} - \frac{d}{dr}p_{20,0} = \alpha^2\mathcal{F}_{P0}, \tag{24a}$$

$$\frac{1}{r^2}\frac{d}{dr}\left(r^2 u_{20,0}\right) = 0, \tag{24b}$$

$$\frac{d^2}{dr^2}u_{20,2} + \frac{2}{r}\frac{d}{dr}u_{20,0} - 8\frac{u_{20,2}}{r^2} + \frac{2\sqrt{6}}{r^2}v_{20,2} - \frac{d}{dr}p_{20,2} = \alpha^2\mathcal{F}_{P2}, \tag{24c}$$

$$\frac{d^2}{dr^2}v_{20,2} + \frac{2}{r}\frac{d}{dr}v_{20,2} - \frac{6}{r^2}v_{20,2} + \frac{2\sqrt{6}}{r^2}u_{20,2} - \frac{\sqrt{6}}{r}p_{20,2} = \alpha^2\mathcal{F}_{B2}, \tag{24d}$$

$$\frac{d}{dr}u_{20,2} + \frac{2}{r}u_{20,2} - \frac{\sqrt{6}}{r}v_{20,2} = 0. \tag{24e}$$

This system is subject to **homogeneous boundary conditions at $r = 1$** and **regularity conditions at $r = 0$.**

Theoretical model IV

Solution

The solution of (24) subject to the boundary conditions is

$$u_{20,0} = 0, \tag{25a}$$

$$p_{20,0} = P_{20} + \int_0^r -\alpha^2 \mathcal{F}_{P0}(r')dr', \tag{25b}$$

$$u_{20,2} = c_1 r + c_2 r^3 + r I_1(r) + \frac{1}{r^2} I_2(r) + r^3 I_3(r) + \frac{1}{r^4} I_4(r), \tag{25c}$$

$$v_{20,2} = \frac{1}{\sqrt{6}} \left(3c_1 r + 5c_2 r^3 + 3r I_1(r) + 5r^3 I_3(r) - \frac{2}{r^4} I_4(r) \right), \tag{25d}$$

where P_{20} is an arbitrary constant, we omit the expression for $p_{20,2}$ and

$$c_1 = -I_1(1) - \frac{5}{2} I_2(1) - \frac{7}{2} I_4(1), \quad c_2 = \frac{3}{2} I_2(1) - I_3(1) + \frac{5}{2} I_4(1).$$

where

$$I_1 = -\frac{\alpha^2}{10} \left(r\mathcal{F}_{P2}(r) - 2\int_0^r \mathcal{F}_{P2}(r')dr' \right), \quad I_2 = \frac{\alpha^2}{10} \left(r^4 \mathcal{F}_{P2}(r) - 5\int_0^r \mathcal{F}_{P2}(r') r'^3 dr' \right), \tag{26a}$$

$$I_3 = \frac{3\alpha^2}{70} \left[\frac{\mathcal{F}_{P2}(r')}{r'} \right]_0^r, \qquad I_4 = -\frac{3\alpha^2}{70} \left(r^6 \mathcal{F}_{P2}(r) - 7\int_0^r \mathcal{F}_{P2}(r') r'^5 dr' \right). \tag{26b}$$

Theoretical model V

Steady streaming velocity and streamfunction

$$\mathbf{u}_{20} = \left(\frac{1}{4}\sqrt{\frac{5}{\pi}}\, u_{20,2}(3\cos^2\theta - 1), -\frac{1}{4}\sqrt{\frac{30}{\pi}}\, v_{20,2}\cos\theta\sin\theta, 0 \right),$$

$$\psi_{20} = \frac{1}{4}\sqrt{\frac{5}{\pi}}\, r^2 u_{20,2}\sin^2\vartheta\cos\vartheta, \quad \text{where } \mathbf{u}_{20} = \boldsymbol{\nabla} \times \left(\frac{\psi_{20}}{r\sin\vartheta}\hat{\boldsymbol{\varphi}} \right).$$

The integrals (26) do not admit an analytical solution and need to be computed numerically.

Theoretical model VI

Limiting cases that allow for analytical solutions

Small α

$$\psi_{20} = \frac{\alpha^6}{415800} r^3 (1-r^2)^2 (2+r^2) \sin^2\vartheta \cos\vartheta + O(\alpha^8),$$

$$\mathbf{u}_{20} = \frac{\alpha^6}{415800} \left[r(1-r^2)^2(2+r^2)(3\cos^2\vartheta - 1) - 3r(1-r^2)(2-3r^2-3r^4)\sin\vartheta\cos\vartheta, 0 \right] + O(\alpha^8).$$

- In the limit $\alpha \to 0$ the fluid moves as a rigid body and the steady streaming tend to vanish.
- As $\alpha \to 0$w the intensity of the steady streaming is proportional to α^6.

Large α

$$\psi_{20} = \frac{1}{8} r^3 (1-r^2) \sin^2\vartheta \cos\vartheta + \mathcal{O}\left(\frac{1}{\alpha}\right), \tag{27a}$$

$$\mathbf{u}_{20} = \left(\frac{1}{8} r(1-r^2)(3\cos^2\vartheta - 1), -\frac{1}{8}(3r - 5r^3 + \frac{2}{r^3} e^{-\sqrt{2}\alpha(1-r)}) \cos\vartheta \sin\vartheta, 0 \right) + \mathcal{O}\left(\frac{1}{\alpha}\right). \tag{27b}$$

- The final term in the ϑ-component of $\mathbf{u}_{20}$ decays rapidly far from the wall and ensures the no slip condition is satisfied.
- This means that the steady streaming flow also has a boundary layer at $r = 1$ for large α.

Experimental measurement of the steady streaming

- The steady streaming flow can be direclty measured experimentally by cross-correlating images that are separated in time by a multiple of the frequency of oscillation.
- This procedure filters out from the measurements the oscillatory component of the flow.

Comparison between experimental and theoretical results I

Repetto et al. (2008), J. Fluid Mech.

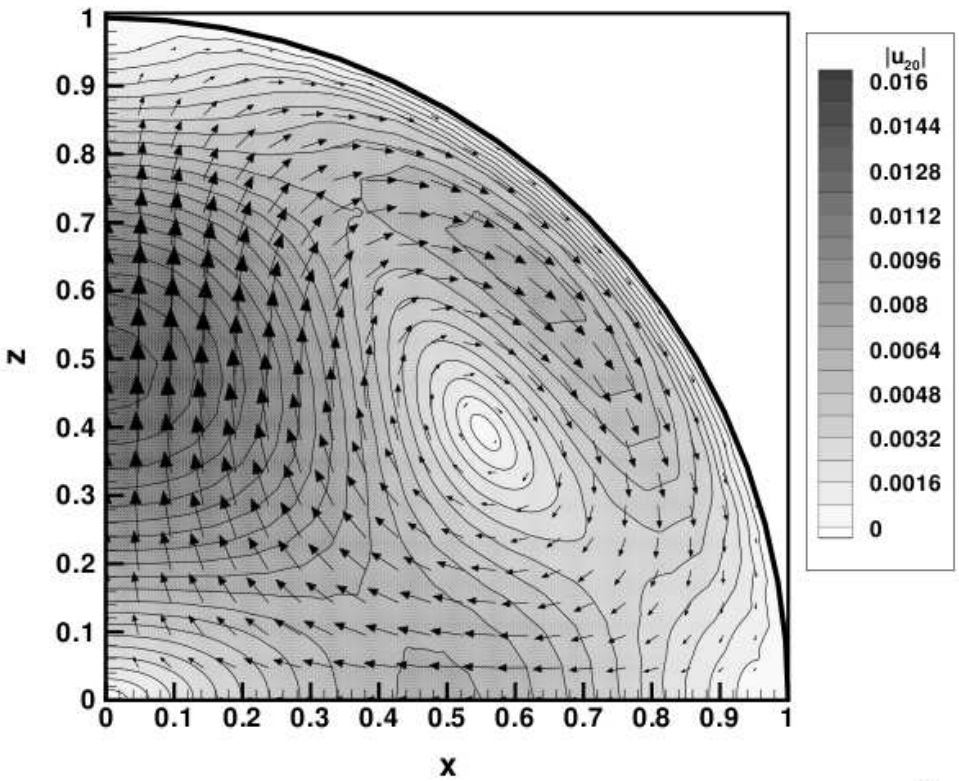

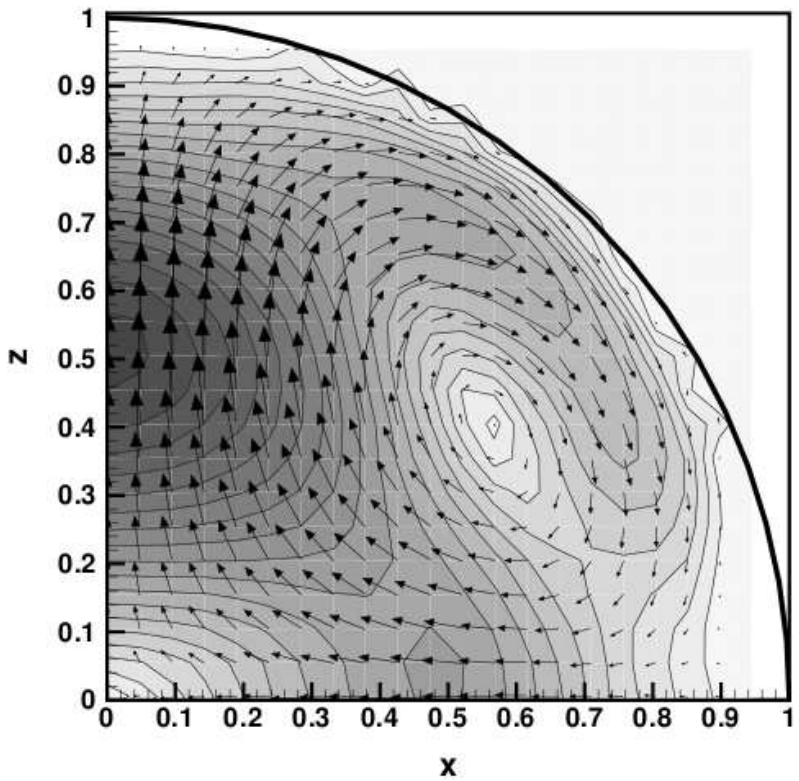

Comparison between experimental and theoretical results II

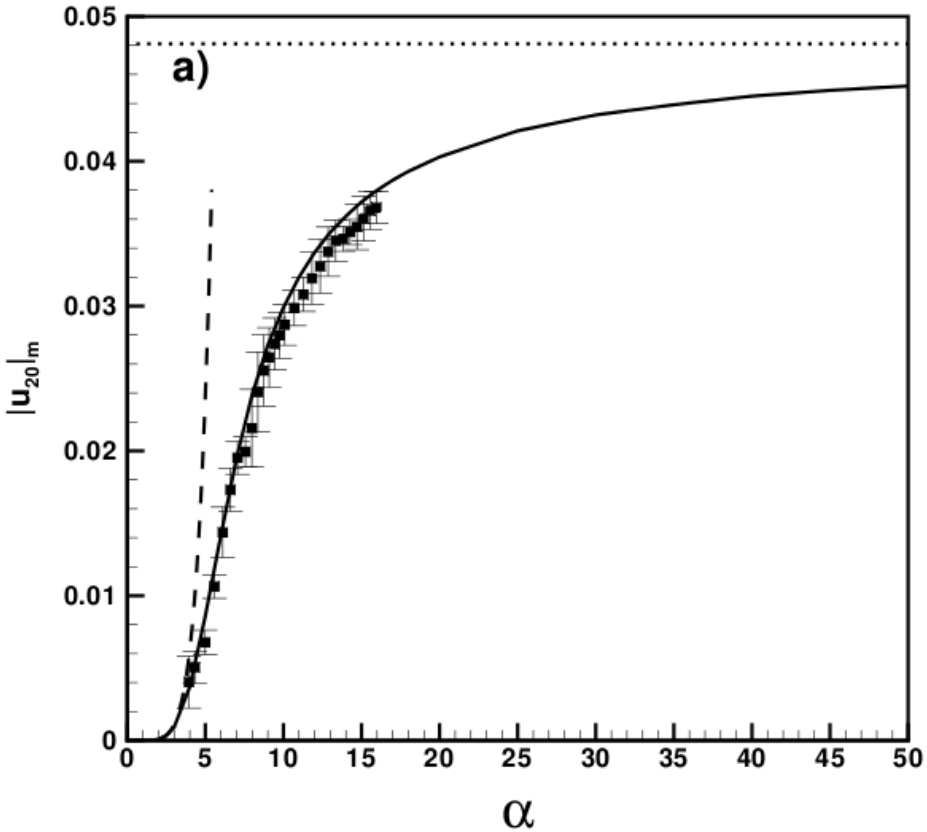

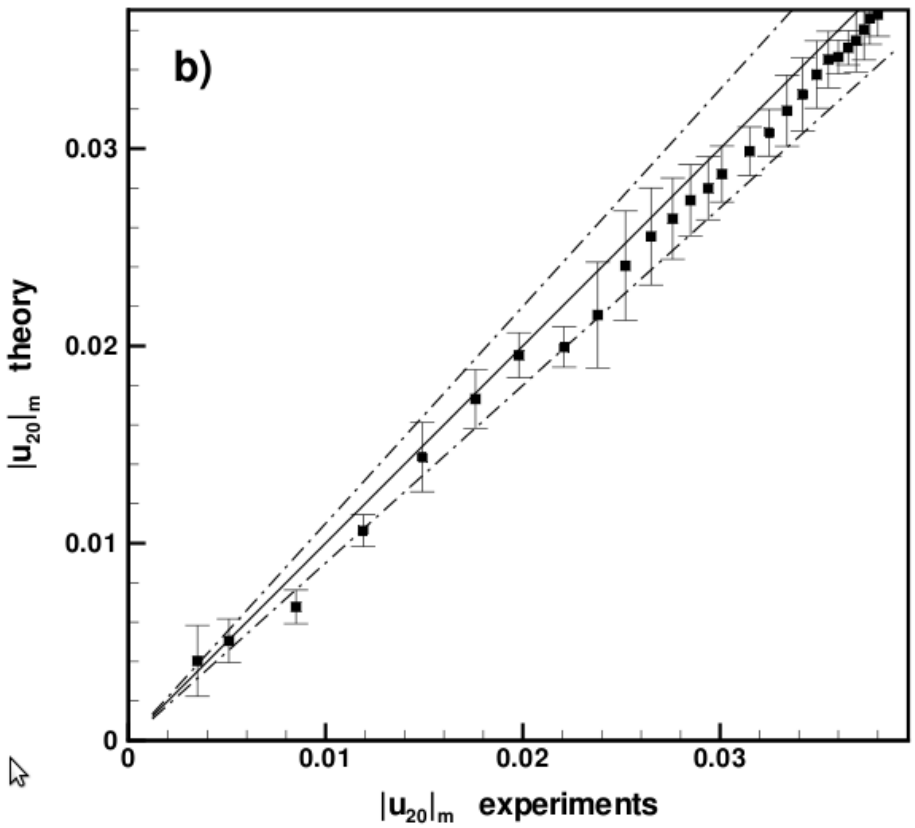

a) Intensity of the steady streaming flow versus the Womersley number α.
b) Comparison between experimental and theoretical results in terms of steady streaming intensity.

Comparison between experimental and theoretical results III

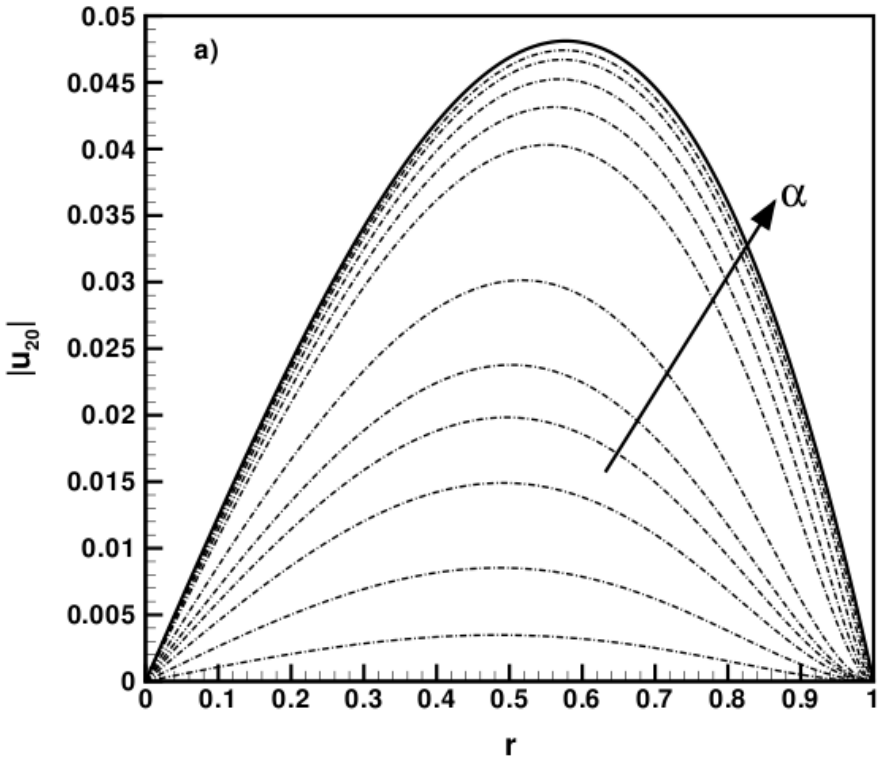

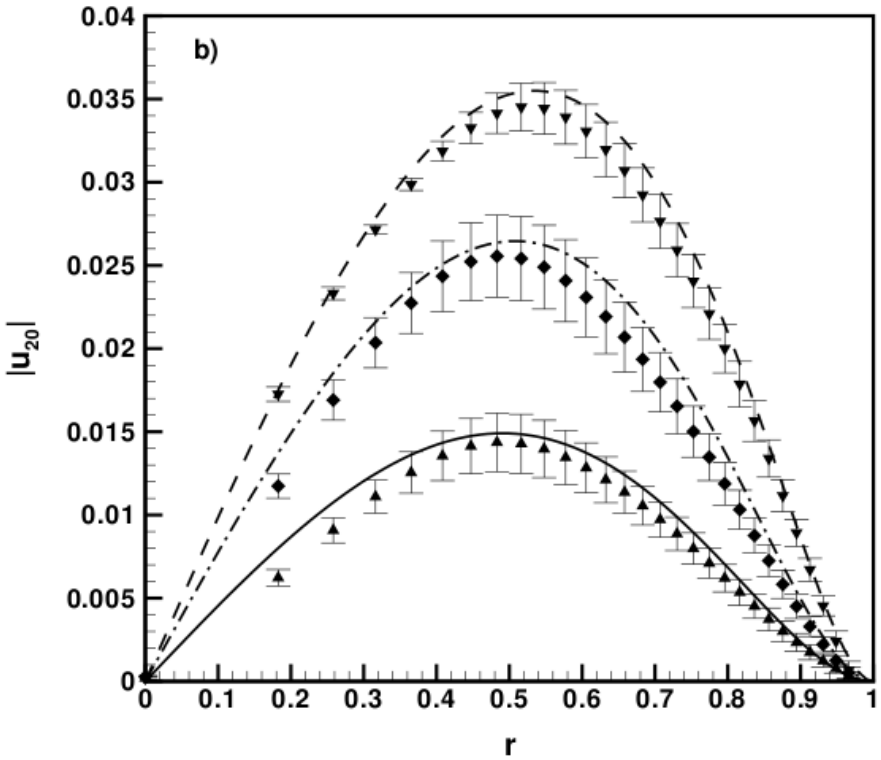

a) Radial velocity profiles on the equatorial plane for different values of the Womersley number α.
b) Comparison between experimental and theoretical results in terms of radial velocity profiles.

Effect of the geometry on the steady streaming

Non-sphericity of the domain

- The antero-posterior axis is shorted than the others;
- the lens produces an anterior indentation.

What is the effect of the geometry on the steady streaming?

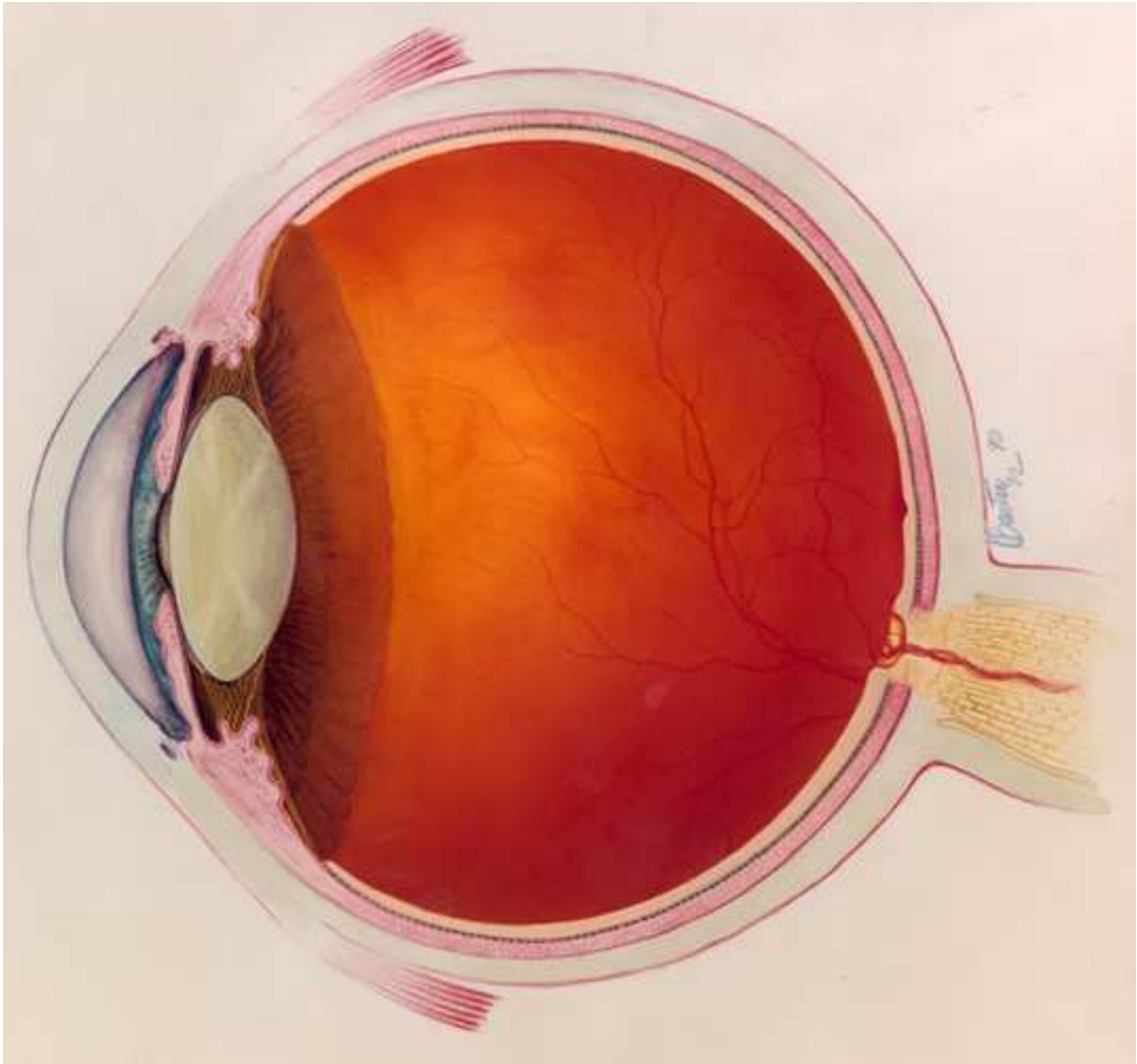

Theoretical model I

Repetto et al. (2010), Biomech. Model. Mechanobiol.

We assume small amplitude sinusoidal torsional oscillations

$$\beta = -\varepsilon \cos(\omega_0 t^*) \qquad \varepsilon \ll 1.$$

Scaling

$$\mathbf{u} = \frac{\mathbf{u}^*}{\omega_0 R_0}, \quad t = t^* \omega_0, \quad (r, R) = \frac{(r^*, R^*)}{R_0}, \quad p = \frac{p^*}{\mu \omega_0}.$$

Dimensionless governing equations

$$\alpha^2 \left(\frac{\partial}{\partial t} - \varepsilon \sin t \frac{\partial}{\partial \varphi} \right) \mathbf{u} + \alpha^2 (\mathbf{u} \cdot \nabla) \mathbf{u} + \nabla p - \nabla^2 \mathbf{u} = 0, \tag{28a}$$

$$\nabla \cdot \mathbf{u} = 0, \tag{28b}$$

$$u = v = 0, \; w = \varepsilon R \sin\vartheta \sin t \qquad [r = R(\vartheta, \varphi)], \tag{28c}$$

Shape of the domain

We write the function $R(\vartheta, \varphi)$ describing the shape pf the domain as

$$R(\vartheta, \varphi) = 1 + \delta R_1(\vartheta, \varphi), \qquad \delta \ll 1.$$

Theoretical model II

Expansion

We seek a series solution to (28a-c) by expanding in ascending powers of the small parameters ε and δ:

$$\mathbf{u} = \varepsilon\left(\mathbf{u}_{10} + \delta\mathbf{u}_{11} + \dots\right) + \varepsilon^2\left(\mathbf{u}_{20} + \delta\mathbf{u}_{21} + \dots\right) + \dots,$$
$$p = \varepsilon\left(p_{10} + \delta p_{11} + \dots\right) + \varepsilon^2\left(p_{20} + \delta p_{21} + \dots\right) + \dots.$$

- **Problem at $\mathcal{O}(\varepsilon)$:** leading order flow in a sphere.
- **Problem at $\mathcal{O}(\varepsilon\delta)$:** perturbation of the flow in the sphere due to the geometry.
- **Problem at order $\varepsilon^2\delta^0$:** steady streaming in a sphere.
- **Problem at order $\varepsilon^2\delta$**
  At this order we can write

$$\mathbf{u}_{21} = \mathbf{u}_{21}^{(0)} + \mathbf{u}_{21}^{(2)} e^{2it} + \overline{\mathbf{u}_{21}^{(2)}} e^{-2it}, \quad p_{21} = p_{21}^{(0)} + p_{21}^{(2)} e^{2it} + \overline{p_{21}^{(2)}} e^{-2it}.$$

  We consider here the perturbation in the steady streaming due to the geometry of the domain, which is given by $\mathbf{u}_{21}^{(0)}$ and $p_{21}^{(0)}$. The details of the solution are skipped.

Theoretical model III

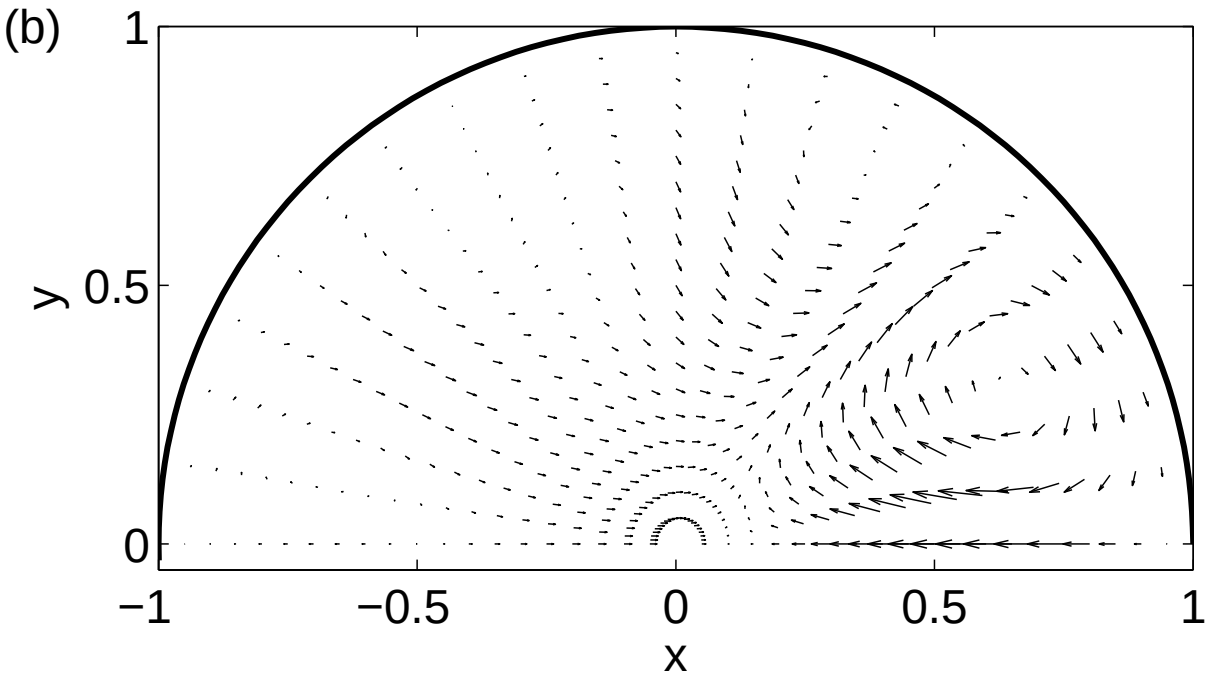

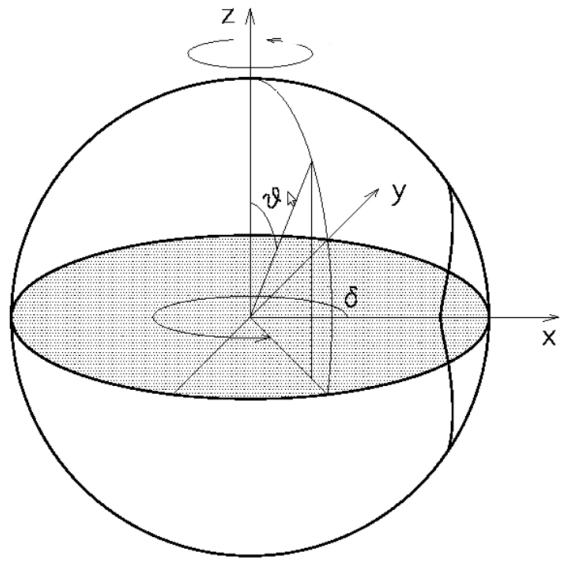

Perturbation of the steady streaming flow on the equatorial plane

Experimental measurement of the steady streaming flow

$\alpha = 3.8$

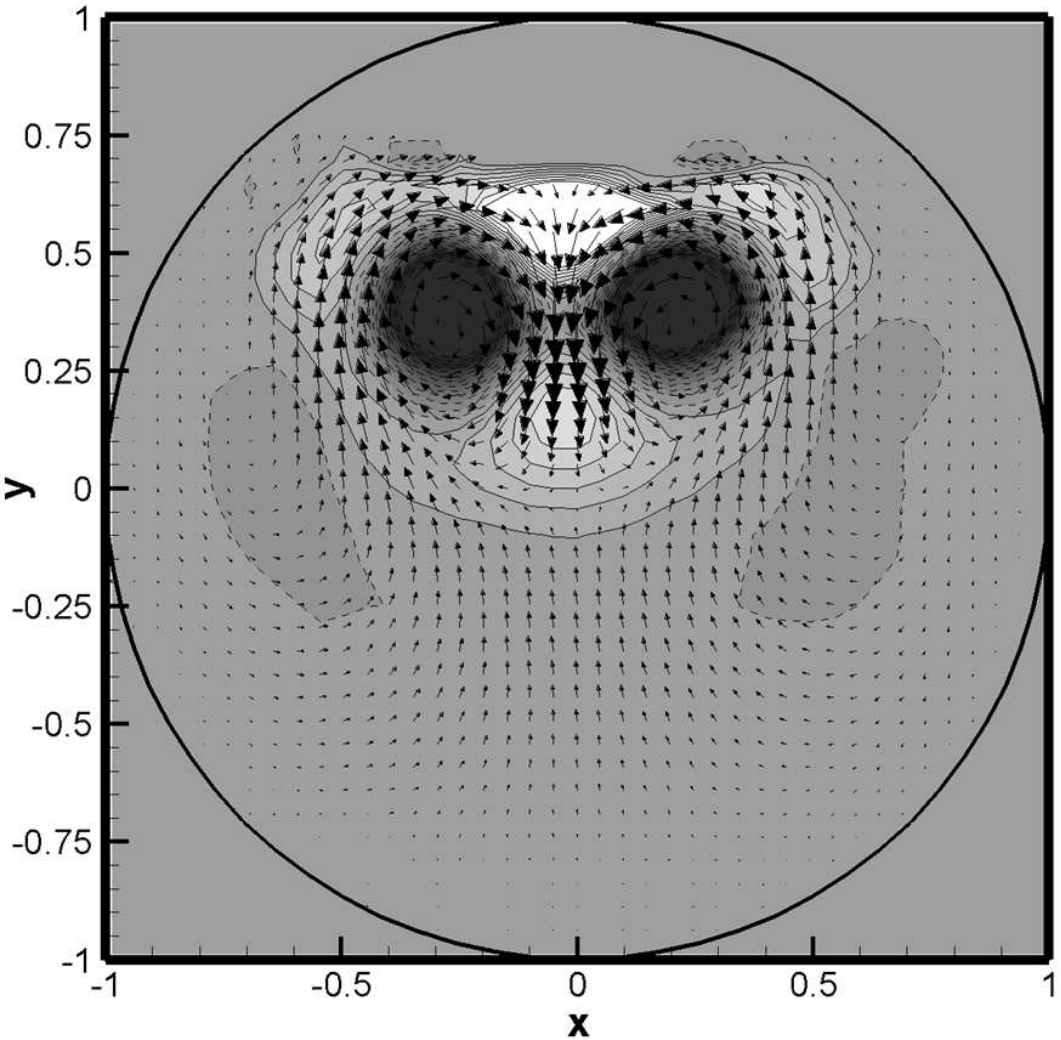

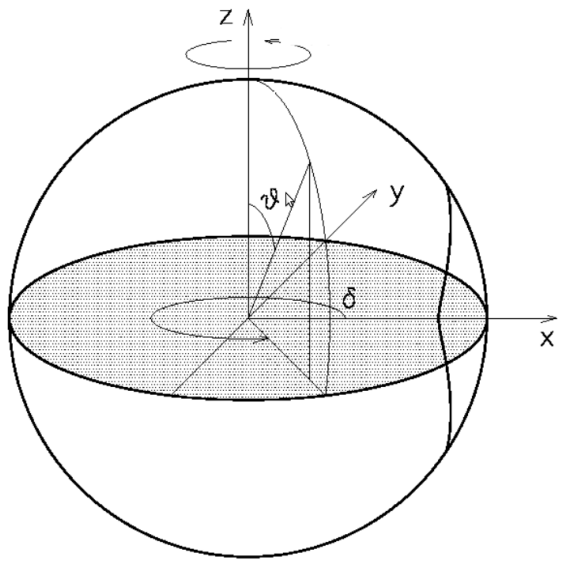

Steady streaming flow on the equatorial plane.

Conclusions

- Eye movements during reading: $\approx$ 0.16 rad, $\approx 63\ s^{-1}$ (Dyson et al., 2004).
- Kinematic viscosity of the vitreous: $\nu \approx 7 \times 10^{-4}$ m^{2}s^{-1} (Lee et al., 1992).
- Eye radius: $R_0 = 0.012$ m.
- Womersley number: $\alpha = 3.6$.
- Streaming velocity: $U = \varepsilon^2 \delta \max(|\mathbf{u}_{21}^{(0)}|) \approx 6 \times 10^{-5}$ m s^{-1}.
- Diffusion coefficient of fluorescein: $D \approx 6 \times 10^{-10}$ m s^{-1} (Kaiser and Maurice, 1964)

Peclèt number: $Pe \approx 1200$.
In this case advection is much more important than diffusion!

Work in progress

Julia Meskauskas

- **Steady streaming in a viscoelastic fluid.**
- **Stress on the retina during real eye movements.**
- **Non-homogeneous vitreous properties.**

Andrea Bonfiglio

- **Experimental study of vitreous mixing.**
- **Experimental study with viscoelastic fluids.**

In collaboration with **Amabile Tatone.**

- **Motion of the vitreous after Posterior Vitreous Detachment.**

  The gel phase is modelled as a hyperelastic viscous solid, the liquefied vitreous as a viscous fluid.

- **Quasi static shrinking of the vitreous.**

References I

D. A. Atchison, N. Pritchard, K. L. Schmid, D. H. Scott, C. E. Jones, and J. M. Pope. Shape of the retinal surface in emmetropia and myopia. *Investigative Ophthalmology & Visual Science*, 46(8):2698–2707, 2005. doi: 10.1167/iovs.04-1506.

W. Becker. Metrics. In R. Wurtz and M. Goldberg, editors, *The neurobiology of saccadic eye movements*. Elsevier Science Publisher BV (Biomedical Division), 1989.

T. David, S. Smye, T. Dabbs, and T. James. A model for the fluid motion of vitreous humour of the human eye during saccadic movement. *Phys. Med. Biol.*, 43:1385–1399, 1998.

R. Dyson, A. J. Fitt, O. E. Jensen, N. Mottram, D. Miroshnychenko, S. Naire, R. Ocone, J. H. Siggers, and A. Smithbecker. Post re-attachment retinal re-detachment. In *Proceedings of the Fourth Medical Study Group, University of Strathclyde, Glasgow*, 2004.

B. Lee, M. Litt, and G. Buchsbaum. Rheology of the vitreous body. Part I: viscoelasticity of human vitreous. *Biorheology*, 29:521–533, 1992.

J. Meskauskas, R. Repetto, and J. H. Siggers. Oscillatory motion of a viscoelastic fluid within a spherical cavity. *Journal of Fluid Mechanics*, 685:1–22, 2011. doi: 10.1017/jfm.2011.263.

C. S. Nickerson, J. Park, J. A. Kornfield, and H. Karageozian. Rheological properties of the vitreous and the role of hyaluronic acid. *Journal of Biomechanics*, 41(9):1840–6, 2008. doi: 10.1016/j.jbiomech.2008.04.015.

R. Repetto, A. Stocchino, and C. Cafferata. Experimental investigation of vitreous humour motion within a human eye model. *Phys. Med. Biol.*, 50:4729–4743, 2005. doi: 10.1088/0031-9155/50/19/021.

References II

R. Repetto, J. H. Siggers, and A. Stocchino. Steady streaming within a periodically rotating sphere. *Journal of Fluid Mechanics*, 608:71–80, August 2008. doi: 10.1017/S002211200800222X.

R. Repetto, J. H. Siggers, and A. Stocchino. Mathematical model of flow in the vitreous humor induced by saccadic eye rotations: effect of geometry. *Biomechanics and Modeling in Mechanobiology*, 9(1):65–76, 2010. ISSN 1617-7959. doi: 10.1007/s10237-009-0159-0.

K. Swindle, P. Hamilton, and N. Ravi. In situ formation of hydrogels as vitreous substitutes: Viscoelastic comparison to porcine vitreous. *Journal of Biomedical Materials Research - Part A*, 87A(3):656–665, Dec. 2008. ISSN 1549-3296.